International Journal of Computer Research
Volume 24, Number 4
ISSN: 1535-6698

FREQUENCY AND VOLTAGE CONTROL OF MULTI AREA POWER SYSTEM VIA NOVEL PARTICLE SWARM OPTIMIZATION TECHNIQUES*

M. A. Ebrahim[1,2,†] , Ali. M. Ali[3] and M. A. Moustafa Hassan[4]

[1]Department of Electrical Engineering, Faculty of Engineering at Shoubra, Benha University, Cairo, Egypt
[2]FCLab FR CNRS 3539, Belfort, France
[3]Power Station of Cairo North, Ministry of Electricity and Energy, Egypt
[4]Department of Electrical Engineering, Faculty of Engineering, Cairo University, Giza, Egypt

ABSTRACT

The increased demand for the electricity arises request for providing high-quality power with constant voltage and frequency. Moreover, in the interconnected power system, the main desired objective is the high-quality power exchange between areas over interconnecting tie lines. To achieve high quality active and reactive powers, the Load Frequency Control (LFC) and Automatic Voltage Regulator (AVR) should be considered. The desired objectives in this chapter are designing the area LFC to have some degree of control over tie-line power flow and frequency of individual areas and also maintaining a constant voltage over it using AVR. It is important to properly design the area LFC and AVR to improve both the quality and reliability of the electricity delivered to consumers. In the actual power systems, there exist nonlinearities such as parameters variations and Generation Rate Constraints (GRC) for generating units which are considered in this chapter. Accordingly, the controller obtained for LFC as well as AVR based on Particle Swarm Optimization (PSO) are proposed since those techniques are capable of dealing with nonlinear models.

This study proposes both I and PID controllers for LFC and AVR using various types of PSO. A comprehensive comparative study is performed to prove the effectiveness of the proposed PSO based controllers. Simulation results proved the capability of the proposed controllers to deal with small load disturbance as well as a large disturbance in the presence of GRC.

---

* This is a reformatted version of a chapter previously published in: Walker, Brian. *Particle Swarm Optimization (PSO). Advances in Research Applications.* New York: Nova Science Publishers, 2017.

† Corresponding Author E-mail: mohamedahmed_en@yahoo.com

In this chapter, there are different kinds of PSO are introduced like Time-Varying Initial Weight, Constrictive, Adaptive Acceleration Coefficients and Modified Adaptive Acceleration Coefficients Particle Swarm Optimization to obtain the optimal gains.

Keywords: load frequency control, automatic generation control, automatic voltage regulator, proportional integral derivative (PID), particle swarm optimization (PSO)

INTRODUCTION

Nowadays, every person needs a continuous power supply with high quality. But it is always not possible for the electrical power grid to stay in normal steady state, a power plant control system got to observe the load conditions and supply consumers a whole day. It is, therefore, unrelated to consider that consistent power is generated throughout. In view of the fact that both the active and reactive power requests are continual changes with falling and rising trend [1, 2]. In modern interconnected networks, where a number of areas are interconnected and power is alternated between them over tie-lines, the LFC and AVR systems are the main requirements.

The aims of LFC are to share the load between generators and to control the tie-line power to pre-define values and to maintain suitable uniform frequency. So as to supply reliable electric power with good quality, LFC in power system is very important. Regular frequency is specified as the mark of a normally operating system.

In a modern interconnected power system, manual control is not possible. Therefore, automatic equipment is installed on each generator. So based on the load, the power generation varies. The purpose of the control strategy is to deliver and generate power in an interconnected system as consistently and economically as possible whereas maintaining the frequency and voltage within the limits.

The system frequency is essentially influenced due to change in load, whereas reactive power based on changes in voltage magnitude and is less affected by frequency. To remain the frequency constant Integral and Proportional-integral-Derivative (PID) controller is used which controls the turbines used for tuning the generators and in addition the steady state error of systems frequency is minimized by tuning the controller gains.

Excitation of the generator must be regulated in order to match the reactive power require, if not the bus voltage falls outside the allowed limit. The mechanical input power to the generator is used to control the frequency of electrical power production and to keep the power exchange between the areas as scheduled.

With the aim of getting better performance from any controller, its parameters require good optimization. The conventional methods face some problems to achieve this purpose, like complex mathematical equations for large systems [3].

Evolutionary Computations (EA) techniques present some challenges for parameters optimization of controllers.

There are different algorithms of EA to optimize the controller gains of an interconnected power system such as Genetic Algorithm (GA) but this one has problems to implement due to its complexity in coding and low speed of convergence. Another method is Artificial Bee Colony Optimization algorithms (ABC) deals with the problem of reproduction process which gives rise to a population of N individuals. Here in this research, a various types of Particle Swarm Optimization (PSO) is used for tuning the proposed controllers of LFC and AVR in addition to non-linearity of system is applied to single area LFC with/without AVR and two areas LFC with/without AVR due to its simplicity and is not affected size of problem and successfully solves large-scale non-linear optimization tribulations.

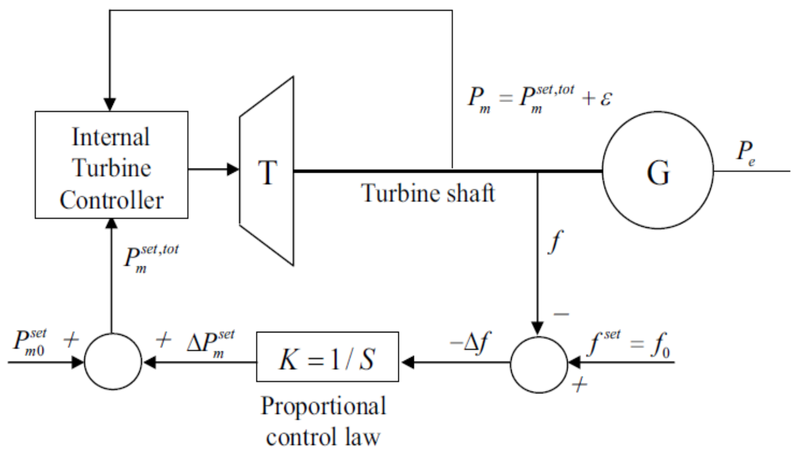

Figure 1. Primary Control Block Diagram.

LFC System Modeling

The LFC is to control the frequency variation through keeping the real power balance in the system. The main functions of LFC are to keep the constant frequency with growing load change, control the tie-line flows and divided the load between the participating generation units. The automatic control system for LFC forms of two central parts, the primary and secondary control. Tertiary control, which is manual, activated corresponding to the electricity production according to generations' schedules (dispatch).

Primary Frequency Control

The control task of it is to return the frequency back (in short time) to suitable values but there remains an inescapable frequency control error because the control law is only proportional therefore there is necessity to secondary frequency control to eliminate this error, it's noted that S is called speed droop (in some books called R [4]) or a regulation constant [5] (Hz/unit).

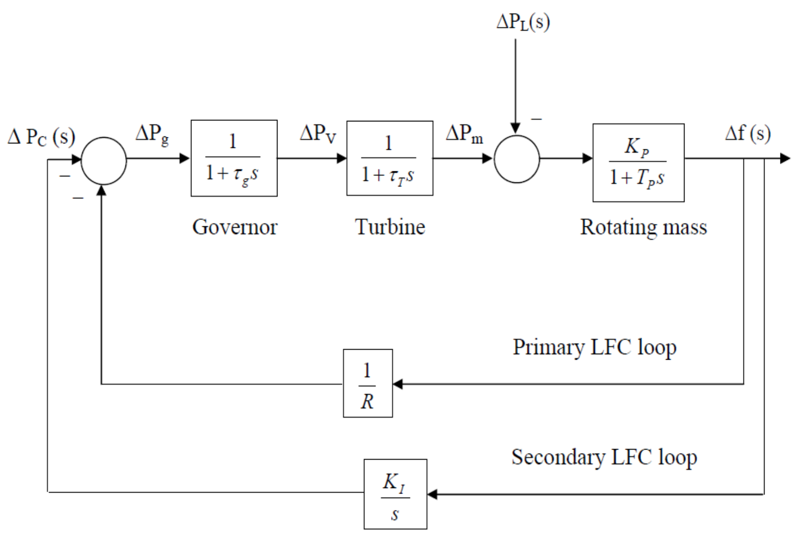

Figure 2. Block Diagram of LFC for Single-Area System with Primary and Secondary Control Loops.

SECONDARY FREQUENCY CONTROL

Now it had been realized that normal speed will not be the set point because of primary controller, and there will be an offset. One method to restore the speed or frequency to its normal value is to add an integrator. The integral term observes the average error among a period of time and will overcome the offset. Because of its ability to restore a system to its set point, the integral action also identified as the rest action. Hence, as the system load changes continuously, the generation is tuning to restore the frequency to the desired value. This plan is done manually through LFC or Automatic Generation Control (AGC).

Reminder that the primary and secondary control, are continuously actives too in normal operation of the grid to compensate for small fluctuations. Figure 2 represents a block diagram of LFC for single area power system with the primary and secondary load frequency controls.

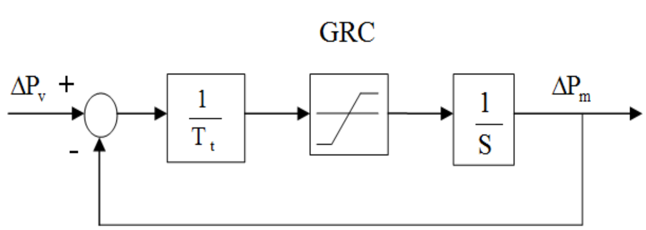

Figure 3. Nonlinear Turbine Model with GRC.

GENERATION RATE CONSTRAINT

In actual power systems, there is a maximum limit on the rate of the change in the generation power as presented in Figure 3. The Generation Rate Constraint (GRC) is considered by adding a limiter to the turbine and the integral control part to avoid excessive control action [6]. In the case where GRC is considered, the system will show larger settling times and longer overshoots, contrasted with the case where GRC is not considered. Classic value for GRC is supposed as 0.1 p.u MW/min [7], where 1 p.u MW equals the total rated capability of the generation units feeding the loads.

GENERATOR VOLTAGE CONTROL SYSTEM

From our investigation in LFC, it's observed that if the active power balance is not stable, the frequency in the system will be affected, while an incorrect reactive power balance will result in variations of the voltages in the system from the desired ones. These days, AVR system is usually applied to the power generation units to solve this control problem [8].

The purpose of this control is to keep the system voltage between limits through adjusting the excitation of the machines. The automatic voltage regulator measures the difference between a rectified voltage derived from the stator voltage and the set point voltage.

The voltage of the generator is proportional to flux (excitation) of the generator. The excitation using to control the voltage so the voltage control system is too called as excitation control system or AVR. For the generators, the excitation is introduced by a device (static device or another machine) called the exciter [9]. A rise in the reactive power load of the generator is coming with a drop in terminal voltage magnitude. The voltage magnitude is measured via a potential transformer on one phase. This voltage is rectified and compared to a DC reference set point signal. The amplified error signal adjusts the exciter field and exciter terminal voltage. Hence, the generator field current is increased which leads to an increase in generated e.m.f. The reactive power generation is making a new equilibrium, raising the terminal voltage to the desired value [10]. A rise in the reactive power load of the generator is coming with a drop in terminal voltage magnitude. The voltage magnitude is measured via a potential transformer on one phase. This voltage is rectified and compared to a DC reference set point signal. The amplified error signal adjusts the exciter field and exciter terminal voltage. Hence the generator field current is increased which leads to an increase in generated e.m.f. The reactive power generation is making a new equilibrium, raising the terminal voltage to the desired value [10]. One of the most frequent controllers available commercially is Proportional Integral Derivative (PID) controller. The aim of using the PID controller is to improve the dynamic response, in addition, to decreasing or eliminate the steady state error [11].

The schematic block diagram of AVR with PID controller appears in Figure 4 presented in [12].

AGC INCLUDING AVR SYSTEM MODEL

In view of the fact that there is a weak coupling between LFC and AVR systems, the frequency and voltage were controlled individually. The AGC and AVR loop are regarded as independently because excitation control of generator have small time constant given by field winding, while AGC loop is slow acting loop including major time constant given by turbine and generator moment of inertia.

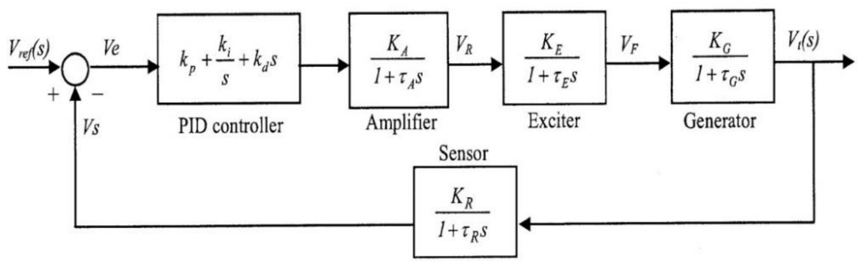

Figure 4. AVR System with PID Controller.

The following linearized equation is obtained:

$$P_e = P_s\Delta\delta + K_2\dot{E} \quad (1)$$

where:

Ps Synchronizing power coefficient.
Δδ The change in the power angle.
K2The change in the electrical power according to a small change in the stator e.m.f.

By applying the small effect of rotor angle upon the generator terminal voltage, can write

$$V_t = K_5\Delta\delta + K_6\dot{E} \quad (2)$$

where:

K_5 The variation in terminal voltage for a small change in rotor angle by constant stator e.m.f.
K_6 The change in terminal voltage for a small change in stator e.m.f by constant rotor angle.

Adding the generator field transfer function with respect to the effect of rotor angle we could state the stator e.m.f as

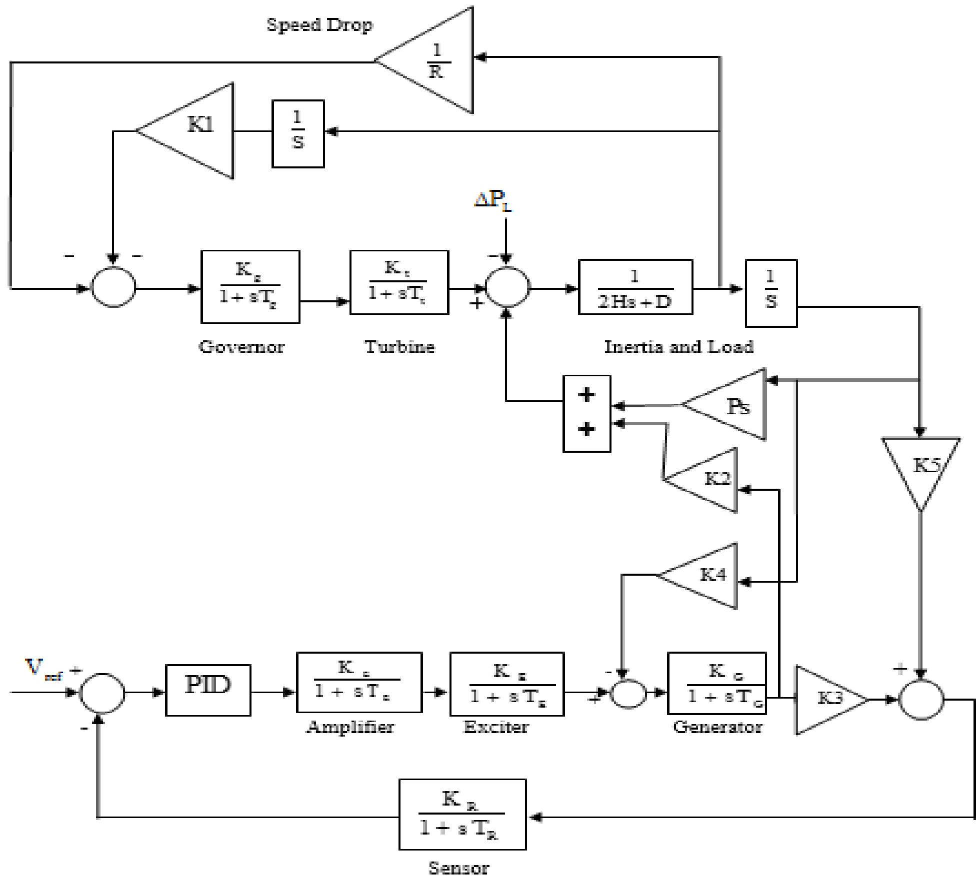

Figure 5. AGC-AVR block diagram of the single area power system.

$$\dot{E} = \frac{K_G}{1+\tau_G s}\left(V_f - K_4\Delta\delta\right) \tag{3}$$

The above constants based upon the network parameters and operating condition also the K_2, K_4 and K_6 are positive gains but K_5 could be negative gain as presented in Figure 5.

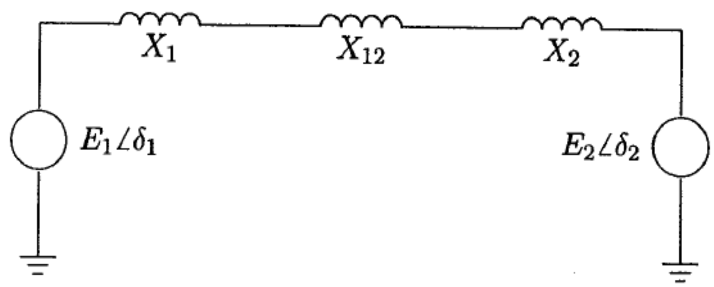

Figure 6. Equivalent System for Two Area Power System.

AGC AND AVR IN MULTI AREA SYSTEM

The main task of multi-area deregulation is to keep zero steady state errors for frequency deviation and fine tracking of the load. In contrast, the power system is supposed to provide the requested dispatch conditions [13]. Consider two areas signified by an equivalent generating unit interconnected through a lossless tie-line with reactance X_{tie}. Each area is represented mathematically by a voltage source with an equivalent reactance as shown in Figure 6. In normal operation, the real power transferred over the tie line is obtained by

$$P_{12} = \frac{|E_1||E_2|}{X_{12}}\sin\delta_{12} \tag{4}$$

where: $X_{12} = X_1 + X_{tie} + X_2$, and δ_1, δ_2 are generator power operating angle where $\delta_{12} = \delta_1 - \delta_2$. Equation (4) can linearize for a small deviation in the tie-line flow ΔP_{12}. From the supposed value can represent as

$$\Delta P_{12} = \frac{dP_{12}}{d\delta_{12}}\Delta\delta_{12} = P_s\Delta\delta_{12} \tag{5}$$

where: P_s is the slope of the power angle curve at the initial operating angle $\delta_{12o} = \delta_{1o} - \delta_{2o}$

The last equation (5) can define by

$$P_s = \frac{dp}{d\delta})_{\delta_0} = P_{max}\cos\delta_0 \tag{6}$$

where: the Pmax cos δ_o is called the slope of the power angle curve at δ_o. It is known as the synchronizing coefficient, indicated by P_s. This coefficient is important in determining the system stability. Therefore we have

$$P_{12} = \frac{dP_{12}}{d\delta_{12}})\delta_{12o} = \frac{|E_1||E_2|}{X_{12}} \cos \delta_{12o} \tag{7}$$

The tie-line power deviation then can represent in the form

$$\Delta P_{12} = P_s(\Delta\delta_1 - \Delta\delta_2) \tag{8}$$

The tie-line power flow shows as a load rise in one area and a load reduce in the other area, based on the direction of the flow. The direction of flow is caused by the phase angle difference; if $\Delta\delta_1 > \Delta\delta_2$, the power flows from area 1 to area 2.

Let us assume a load change ΔP_{L1} in area 1. In the steady state, both areas will have the same steady state frequency deviation

$$\Delta\omega = \Delta\omega_1 = \Delta\omega_2 \tag{9}$$

and

$$\Delta P_{m1} - \Delta P_{12} - \Delta P_{L1} = \Delta\omega\, D_1 \quad \text{and} \quad \Delta P_{m2} + \Delta P_{12} = \Delta\omega\, D_2 \tag{10}$$

The change in mechanical power is obtained by the governor speed characteristics, given by

$$\Delta P_{m1} = \frac{-\Delta\omega}{R_1} \text{ and } \Delta P_{m2} = \frac{-\Delta\omega}{R_2} \tag{11}$$

Substituting from (10) into (11), and solving for $\Delta\omega$,we have

$$\Delta\omega = \frac{-\Delta P_{L1}}{\left(\frac{1}{R_1}+D_1\right)+\left(\frac{1}{R_2}+D_2\right)} = \frac{-\Delta P_{L1}}{B_1+B_2} \tag{12}$$

where:

$$B_1 = \left(\frac{1}{R_1} + D_1\right), B_2 = \left(\frac{1}{R_2} + D_2\right) \tag{13}$$

B_1 and B_2 area known as the frequency bias factors. The change in the tie line power is

$$\Delta P_{12} = -\frac{\left(\frac{1}{R_2}+D_2\right)\Delta P_{L1}}{\left(\frac{1}{R_1}+D_1\right)+\left(\frac{1}{R_2}+D_2\right)} = \frac{B_2}{B_1+B_2}(-\Delta P_{L1}) \tag{14}$$

In the normal operating state, the power system is operated so that the requests of areas area satisfied at the supposed frequency.

The main aims of the multi-area power system are

a) Reduce power system frequency deviation.
b) Interchange power within the fixed range.
c) Control the tie-line power flow at the scheduled value determined [13-16].

Conventional LFC is depending upon tie-line bias control; where each area heads for minimize the area control error (ACE) to zero. The control error for each area consists of a linear combination of frequency and tie-line error.

$$ACE_i = \sum_{j=1}^{n} \Delta P_{ij} + K_i \Delta\omega \quad (15)$$

The area bias K_i defines the amount of interaction through a disturbance in the neighboring areas. An overall acceptable performance is achieved when K_i is chosen equal to the frequency bias factor of that area, i.e., $B_i = (1/R_i) + D_i$ therefore, the ACEs for two area system illustrate as

$$ACE_1 = \Delta P_{12} + B_1 \Delta\omega_1 \quad \text{and} \quad ACE_2 = \Delta P_{12} + B_2 \Delta\omega_2 \quad (16)$$

where: ΔP_{12} and ΔP_{21} are departures from scheduled interchanges.

ACEs are known as actuating signals which it's activates modifications in the reference power set points, and when steady state is achieved, ΔP_{12} and $\Delta\omega$ will be zero. The integrator gain constant must be selected small enough so as not to cause the area to go into a chase mode. It can easily extend the tie-line bias control to an n-area system [17].

Two area interconnected power system of a non-reheat thermal plant is presented in Figure 7:
where:

f_i the system frequency (Hz),
R_i the regulation constant (Hz/unit)
T_{Gi} the speed governor time constant(s)
T_{Ti} the turbine time constant(s)
ACE_i the area control error
ΔP_{Di} the load demand change (watt)
ΔP_c the change in speed changer position
ΔP_G the change in governor valve position
K_{Pi} the power system gain
ΔP_{tie} the change in tie line power (watt)

The above model can extend to have two different areas. Each area has its own LFC and AVR modeling parameters such as illustrates in Figure 8.

PARTICLE SWARM OPTIMIZATION

PSO is a stochastic evolutionary computation technique depends on the movement and intelligence of swarms which the particle updates themselves with the internal velocity and goes to converge to the best solution rapidly [12].

These particles "evolve" by assistance and competition between themselves through generations. Each particle changes its flying according to its own experience as long as its companions experience. Each particle, in fact, forms a potential solution to the problem [19]. PSO is a population dependent optimization techniques include some appealing features such as the ease of implementation and the truth that no gradient information is requested. It can be used to solve a wide range of different optimization problems. Such as evolutionary algorithms, PSO technique conducts a search via a population of particles, similar to individuals [20].

PSO is mainly developed through simulation of birds swarm in two dimension space. The position of each bird is represented by XY axis position and the velocity is represented by V_x (the velocity of X axis) and V_y (the velocity of Y axis). Modification of the bird's position is achieved by the position and velocity information. Bird swarm optimizes a specific objective function. Each bird knows its best value called (P_{best}) and its XY position. This information is the identity of personal experiences of each bird as illustrated in [21].

In PSO, the coordinates of each particle indicate a possible solution related with two vectors, the position (x_i) and velocity (v_i) vectors.

In N-dimensional search space $X_i = [x_i^1, x_i^2, \ldots, x_i^N]$ and $V_i = [v_i^1, v_i^2, \ldots, v_i^N]$ are the two vectors related with each particle i.

A swarm contains a number of particles "or possible solutions" that progress (fly) through the suitable solution space to explore optimal solutions. Each particle updates its position depending on its individual best exploration, best swarm global (overall) experience, and its prior velocity vector in relation to the following form [22]:

$$V_i^{k+1} = w \times V_i^k + C_1 \times R_1 \times (Pbest_i^k - X_i^k) + C_2 \times R_2 \times (Gbest - X_i^k) \quad (17)$$

$$X_i^{k+1} = X_i^k + V_i^{k+1} \quad (18)$$

where:

C_1, C_2	Two positive constants (Cognitive, Social).
R_1, R_2	Two randomly generated numbers with a range of [0, 1].

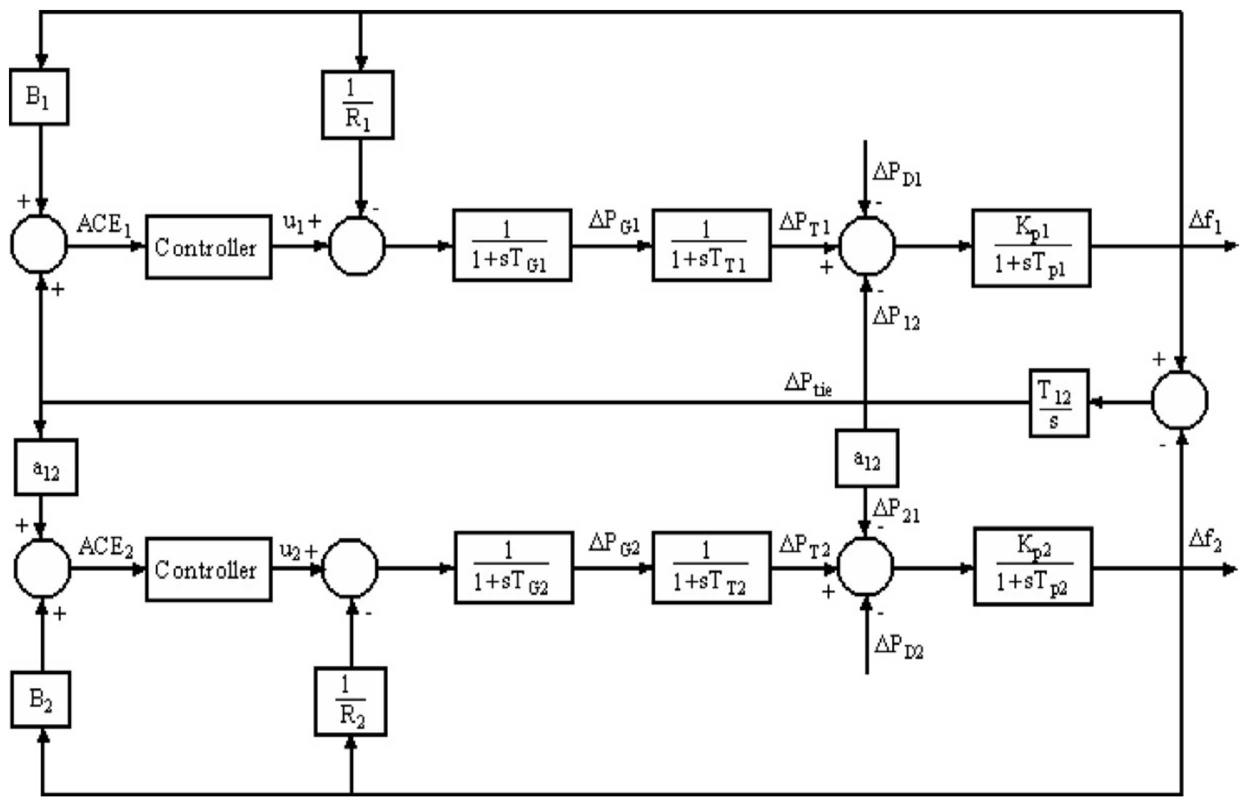

Figure 7. Two area interconnected power system of a non-reheat thermal plant.

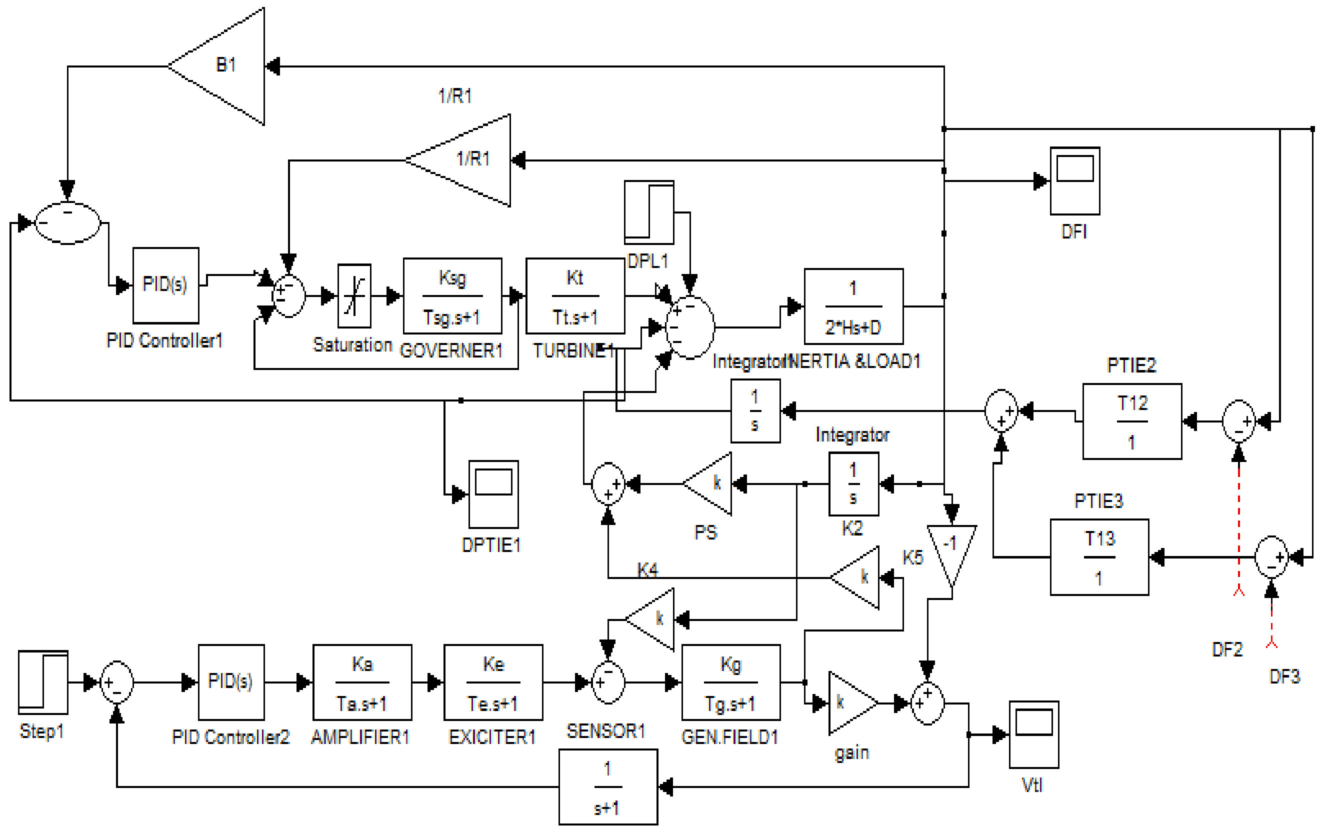

Figure 8. Simplified model of ith areas interconnected system.

w The inertia weight.
P_{besti}^{k} The best position particle accomplished depending on its own experience.
P_{besti}^{k} $[X_{i1}^{pbest}, X_{i2}^{pbest},\ldots, X_{iN}^{pbest}]$
G_{best}^{k} the best particle position based on the whole swarm's experience,
g_{best}^{k} $[X_{i1}^{gbest}, X_{i2}^{gbest},\ldots, X_{iN}^{gbest}]$
k The iteration index.

The expression of P_{best} is called cognitive component whereas the expression of G_{best} called social component, therefore, the values of C_1 and C_2 control the way of each particle in both local and global components, the phrase of $(W \times V_i)$ is previous velocity.

This approach is helpful over evolutionary and genetic algorithm in anyways. First, PSO has memory, therefore, every particle remembers its best solution (global best). In addition to the initial population of the PSO is kept and so there is no necessitate for applying operators to the population, a process that is time and memory-storage-consuming [20].

Figure 9 represents a flow chart of PSO.

CONSTRICTIVE PARTICLE SWARM OPTIMIZATION (C PSO)

The major consideration of constriction factor PSO is to avoid premature convergence of PSO in early stages of search and helps to get away from the local optimal point then improve the convergence of PSO algorithm [23].

$$V_i(k+1) = K\left(V_i(k) \times w + C_1 \times R_1 \times \left(P_{best}(k) - X_i(k)\right) + C_2 \times R_2 \times \left(G_{best}(k) - X_i(k)\right)\right) \tag{19}$$

$$X_i(k+1) = X_i(k) + V_i(k+1) \tag{20}$$

$$K = \frac{2}{abs\left(2 - C - \sqrt{C^2 - 4 \times C}\right)} \tag{21}$$

where:

K Constrictive factor defined by equation (21).
V_i^k The velocity of the particle (i) at iteration (k) and w is inertia weight factor.

C_1, C_2 Acceleration coefficients.
R_1, R_2 Uniformly distributed random number between 0 and 1.

where $C = C_1 + C_2$, $C > 4$ as represented in [24].

P_best The best position of the particle (i) in expectation of iteration (k).
G_best The best position of the flock until iteration k.

$$w = w_{max} - \frac{(w_{max} - w_{min})}{iter_{max}} \times iter \quad (22)$$

w_{max} is final weight, w_{min} is minimum weight.
iter is current iteration and *iter_max* maximum iteration number.

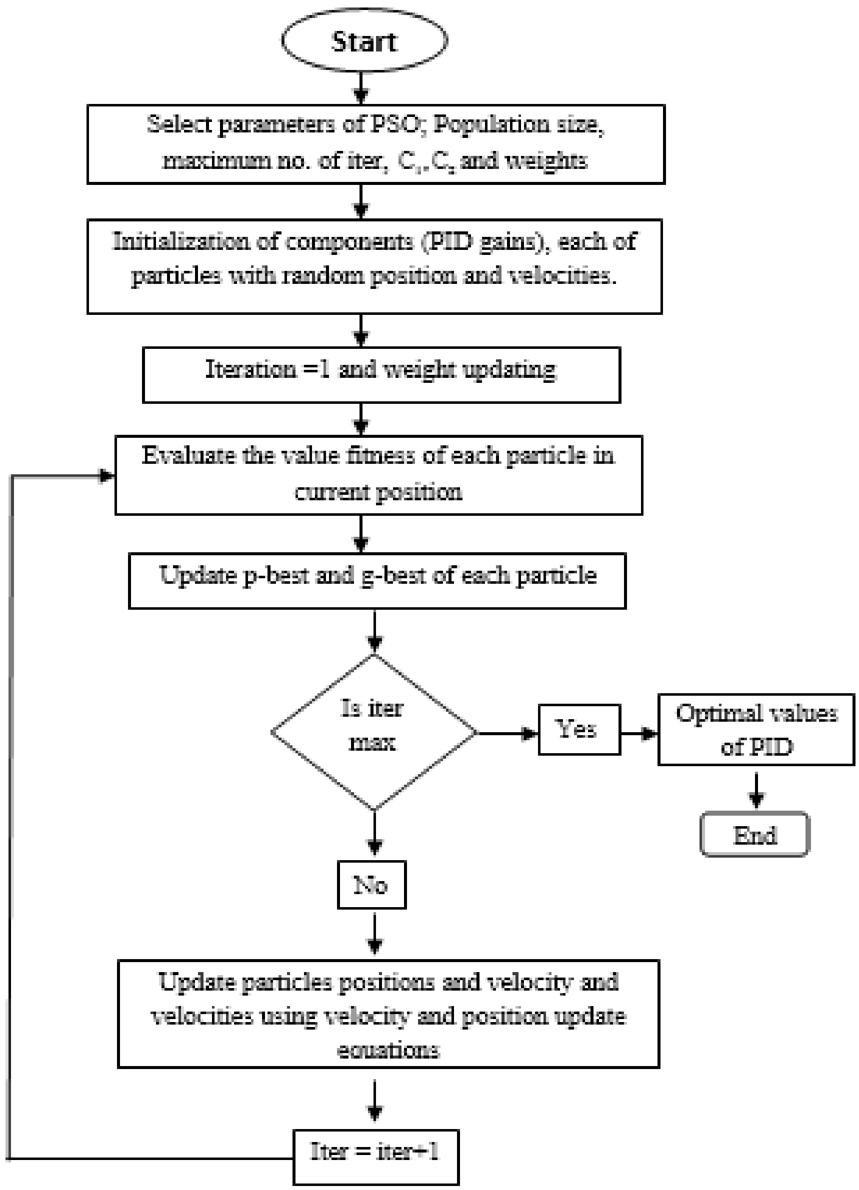

Figure 9. Flow Chart of PSO Algorithm.

A large of inertia weight w at initial searching then linearly decreasing with iteration progressed following equation as

In [25, 26], using PSO with constriction factor and inertia weight (PSO-CF-IW) to solve the economic dispatch of fixed electricity market. The objective function is to reduce the generation price of system accepting the load demand with a limit of constraints such as generation bid quantities, power balance, line limit, ramp rate limits, customer bid quantities, and emission.

TIME-VARYING INERTIA WEIGHT (TVIW) PSO

In the equation (17) it is demonstrated that $V_i(t)$ is a control on exploration and exploitation; therefore the concept of varying (changing) weight (w) is presented for better control of local and global exploration [27].

$$w = w_{max} - \frac{(w_{max} - w_{min})}{t_{max}} \times t \tag{23}$$

where:

w_{max} and w_{min} are final and initial factor weights.
t_{max} is maximum iteration number while t is current iteration number.

But its ability to fine tune the optimum solution is week due to lack diversity at end of the search.

ADAPTIVE ACCELERATION COEFFICIENTS (AAC) PSO

The acceleration coefficients C_1 and C_2 are changed linearly with time that the cognitive component is reduced while social component is increased as search iteration proceeds. The AACPSO changes the acceleration coefficients exponentially in time with respect their minimum and maximum values [27]. The using of exponential function to increase or decrease speed of such function to accelerate the convergence process to get better search in exploration space. Also C_1 and C_2 are adaptively according to the fitness value of G_{best} and P_{best} [27].

$$V_i^{(t+1)} = w^{(t)} V_i^{(t)} + C_i^{(t)} r_1 \times (Pbest_i^{(t)} - X_i^{(t)}) + C_2^{(t)} r_2 \times (Gbest^{(t)} - X_t^{(t)}) \tag{24}$$

where

$$w^{(t)} = w_o.exp(-\alpha_w \times t) \tag{25}$$

$$C_1^{(t)} = c_{1o}.exp(-\alpha_c \times t \times k_c^{(t)}) \tag{26}$$

$$C_2^{(t)} = c_{2o}.exp(\alpha_c \times t \times k_c^{(t)}) \tag{27}$$

$$\alpha_c = -\frac{1}{t_{max}}.ln\left(\frac{c_{2o}}{c_{10}}\right) \tag{28}$$

$$k_c^{(t)} = \frac{(F_m^{(t)} - Gbest^{(t)})}{F_m^{(t)}} \tag{29}$$

where

$C_i^{(t)}$	Acceleration coefficient at iteration where i = 1 or 2.
α_w	calculated respecting to initial and final values of W with the same method as α_c and.
ln	neperian logarithm
$w^{(t)}$	Inertia weight factor.
t	Iteration number.
$k_c^{(t)}$	determined depended on the fitness value of G_{best} and P_{best} at iteration t.
$F_m^{(t)}$	The mean value of the best positions regarding all particles at iteration t.
w_o, C_{oi}	Initial values of inertia weight factor and acceleration coefficients respectively with i = 1 or 2 as represented in [27].

Modified Adaptive Acceleration Coefficients (MAAC) PSO

It is the same equation for (AAC) but it is assumed that $C_1 + C_2 = 4$ so $C_2 = 4 - C_1$. It is supposed to be fewer calculations for C_1 and C_2 then getting faster solutions than (AAC PSO).

IMPLEMENTATION OF PSO-PID CONTROLLER

The design procedures of PSO based PID controller is as follows:

1. Initialize the algorithm parameters such as a number of generation, inertia weight, population, and constants.
2. Initialize the values of the gain parameters K_p, K_i and K_d randomly.
3. Determine the fitness function of each particle in every generation.
4. Determine the local best of every particle and the global best of the particles.
5. Update the position of particle, velocity, local best and global best in each generation.
6. Repeat the steps 3 to 5 until the maximum iteration reached or the best solution is found.

The objective function expresses the function that measures the performance of the system. The fitness function (objective) function for PSO is described as the Integral of Time multiplied by the Absolute value of Error (ITAE) of a system or in several references called the Integral Square Error (ISE). The ISE squares the error to remove negative error terms. Thus, it becomes an unconstrained optimization problem to find a number of decision variables by minimizing the objective function [16, 20, 26].

$$ISE = \sum_{k=1}^{q} e^2(k) \tag{30}$$

PSO minimize the fitness function, the minimization objective function is turned to become as fitness function as follows,

$$f = \frac{1}{ISE} \tag{31}$$

To get the optimum parameters (K_p, K_i, K_d) of PID controller, PSO program has to search in three-dimensional search space. In an ordinary load frequency control systems, while a regulation constant R is used as K_p parameter in PID controller, especially K_i (integral) controller is used in LFC systems. In the submitted system, K_p is put equal regulation constant R also K_i and K_d (integral derivative) controller is used in LFC system. Therefore, for robustness, the regulation constant is tuned corresponding to load and system changes. With the optimized parameters depended on PSO algorithm, the proposed PID controller of the LFC can accomplish optimal properties [28].

EMPIRICAL SETTING AND SIMULATION SCHEMES FOR BENCHMARKS TESTING

Five of the famous benchmarks used in evolutionary optimization methods were used to calculate the performance, both in terms of the optimum solution after a determined number of iterations, and the rate of convergence to the optimum solution, of all the new advancements introduced in this research work, are compared with PSO-TVIW. The performance of all new methods is shown by figures.

All functions have the global minimum at the origin or extremely close to the origin. Simulations were designed to find the global minimum of each function. All benchmarks used are given in Table 1 as given in [29].

Since the majority of the benchmarks used in this research work have the global minimum at or near to the origin of the search space, we use the asymmetric initialization method to examine the performance of the new developments introduced in this research work. The mainly common dynamic ranges used in the literature for the benchmarks assumed in this research were used and the same dynamic range is used in all dimensions [29].

Table 1 presents the range of population initialization and the dynamic range of the search for each function.

Table 1. Benchmarks Functions

Name of the function	Mathematical representation
Sphere function	$f_1(x)=\sum_{i=1}^{n} x_i^2$
Rosenbrock function	$f_2(x)=\sum_{i=1}^{n}\left[100\left(x_{i+1}-x_i^2\right)^2+\left(x_i-1\right)^2\right]$
Rastrigrin function	$f_3(x)=\sum_{i=1}^{n}\left[x_i^2-10\cos\left(2\pi x_i\right)+10\right]$
Griewank function	$f_4(x)=\frac{1}{4000}\sum_{i=1}^{n} x_i^2-\prod_{i=1}^{n}\cos\left(\frac{x_i}{\sqrt{i}}\right)+1$
Schaffer's f6 function	$f_6(x)=0.5-\frac{\left(\sin\sqrt{x^2+y^2}\right)^2-0.5}{\left(1.0+0.001\left(x^2+y^2\right)\right)^2}$

It is perfectly common in PSO to limit the maximum velocity of every modulus to limit unwarranted searching outside the limited search space. Through experimental studies on numerical benchmarks, Eberhart and Shi [30] recommended that it is better to limit the maximum velocity V_{max} to higher than the value of the dynamic range of search X_{max} so, this limitation was used for the simulation in this research.

Table 2. Initialization Range and Dynamic Ranges of the Search for Benchmarks

Function	Range of search	Range of initialization
f_1	$(-100, 100)^n$	$(50, 100)^n$
f_2	$(-100, 100)^n$	$(15, 30)^n$
f_3	$(-10, 10)^n$	$(2.56, 5.12)^n$
f_4	$(-600, 600)^n$	$(300, 600)^n$
f_6	$(-100, 100)^2$	$(15, 30)^2$

Where n is the number of dimensions

Table 3 presents the maximum velocity with the limitation of $V_{max} = X_{max}$ for the benchmarks considered in this research.

Table 3. Maximum Velocity for Benchmarks

Function	Vmax
f_1	100
f_2	100
f_3	10
f_4	600
f6	100

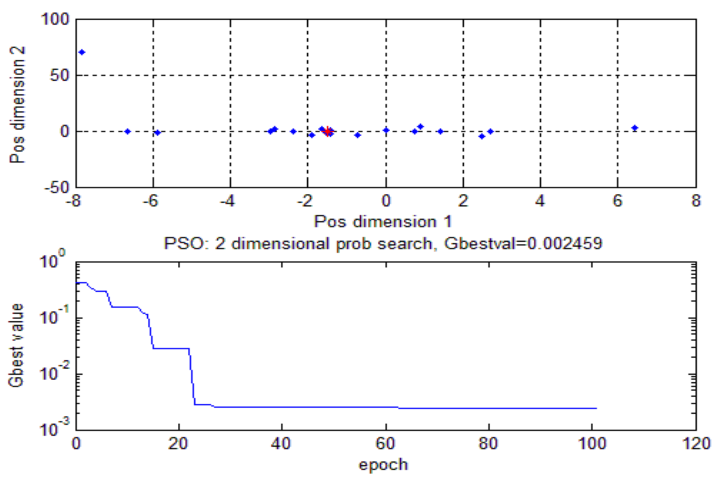

Figure 10. The Objective Function and the Positions of the Particles based on TVIWPSO Gain.

FINDING THE MINIMUM OF THE 'F6' FUNCTION

A further attractive example is the Schaffer f6 function. The function has 2 inputs and one output and seems like a still shot of a pebble dropped into water. It has circular waves that die out as the radius increases. It has a known global minimum at x, y = 0 and the maximum is the first 'wave' around the origin. It has lots of local maximums and minimums making it a good test function for the algorithm [31, 32]. For this purpose, MATLAB-Simulink software is used.

a) Time-Varying Inertia Weight PSO

The Figure 10 presents the objective function and the positions of the particles.
It is observed that TVIWPSO takes 22 epochs (iterations) to get an optimum solution.

b) Constrictive Particle Swarm Optimization

The Figure 11 displays the objective function and the positions of the particles.
It is observed that CPSO takes 30 epochs (iterations) to get the optimum solution.

c) Adaptive Acceleration Coefficients (AACPSO)

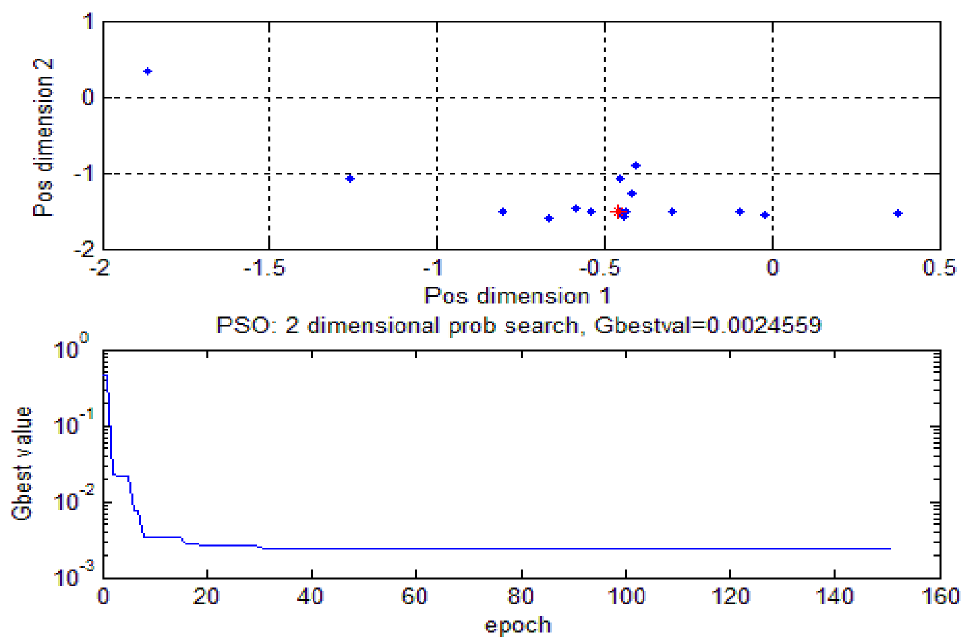

Figure 11. The Objective Function and the Positions of the Particles based on CPSO.

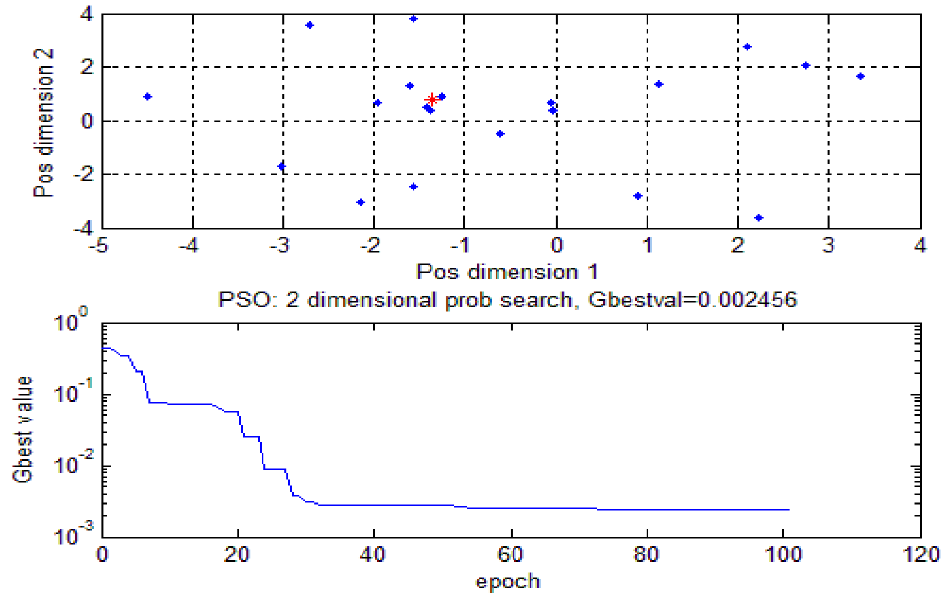

Figure 12. The Objective Function and the Positions of the Particles based on AACPSO.

Table 4. A comparison performance for the four types of PSO

	Number of iterations (epochs)	G_best
TVIWPSO	22	0.002459
C PSO	30	0.002455
AACPSO	30	0.002456
MAACPSO	28	0.002456

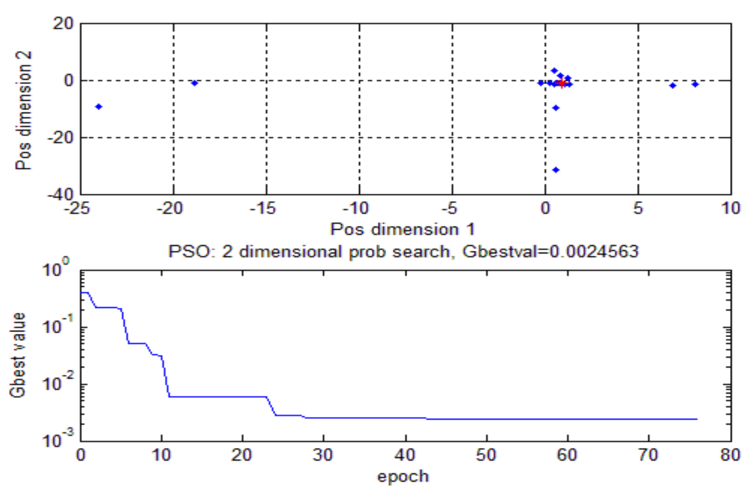

Figure 13. The Objective Function and the Positions of the Particles based on MAACPSO.

The Figure 12 shows the objective function and the positions of the particles. It is observed that AACPSO takes 30 epochs (iterations) to get the optimum solution.

d) Modified Adaptive Acceleration Coefficients (MAACPSO)
The Figure 13 shows the objective function and the positions of the particles.
It is observed that MAACPSO takes 28 epochs (iterations) to get the optimum solution.
In Table 4 illustrates Comparison Performance for the four types of PSO.

CHAPTER ORGANIZATION

The chapter organization has followed the methodological steps to optimize control by using both integral and PID controllers respectively.

A. (Load Frequency Control only).
   1. Load Frequency Control using Integral Controller.
   2. Load Frequency Control with GRC using Integral Controller.
   3. Load Frequency Control with GRC using PID Controller.

B. (Load Frequency Control with Automatic Voltage Control)
   1. LFC with AVR using an integral controller. Using the best integral controller LFC gain from the case (I) in LFC with AVR model to get the PID gain controller of AVR.
   2. LFC with AVR with GRC using an integral controller. Using the best integral controller LFC gain from the case (II) in LFC with AVR model to get the PID gain controller of AVR.
   3. LFC with AVR with GRC using PID controller. Using the best PID controller LFC gains from the case (III) in LFC with AVR model to get the PID gain controller of AVR.

Results of Case Studies in Single Area

Hierarchal of case studies according to chapter structure which introduced in section 9. This section divided to LFC system alone and LFC with AVR systems together.

Load Frequency Control

This section divided LFC into three case studies according to experimental and to obtain the optimal controller. For this purpose, MATLAB-Simulink software is used.

LFC with integral controller (without GRC).

Case under Study

The single area has a single machine (generator and governor) of the non-reheat turbine. By using the model of LFC (with integral gain) was simulated as shown in Figure 14, the turbine rated output is 250 MW at supposed frequency is 50 Hz and sudden load change is 50 MW (ΔP_L = 0.2 per unit) and applying PSO algorithm MATLAB code to optimize and getting the suitable gain.

The parameters of model in Figure 14 are given below:

T_g = 0.2, T_t = 0.5, H = 5, D = 0.8, T_p = 12.5, K_p = 1.25, and R = 0.05.

Table 5 illustrates the most optimal gains obtained by different types of PSO.

Note that these values in Table 5 are taken with tolerance ±2% of full scale.

Table 5. Performance evaluation of various integral gains obtained using different types of PSO

	Integral gain	Objective function	Settling time	Peak value
TVIWPSO	6.4196	11.97516	13.722	0.001421
CPSO	7.3763	0.0012	13.548	0.0014131
AACPSO	6.7958	121.03	13.649	0.0014179
MAACPSO	7.662	5977.9	13.504	0.0014108

Table 6. The Performance and values of integral gain with different types of PSO

	Integral Gain	Objective Function	Settling Time	Peak Value
TVIWPSO	1.6113	0.0557	72.405	0.0023563
CPSO	1.3584	0.1060	72.675	0.00235633
AACPSO	0.6450	170	70.713	0.0023564
MAACPSO	0.5765	848.32	70.713	0.0023564

The Figure 15 illustrates the frequency deviation comparison between different PSO gains of a single area with Integral controller without using GRC.

It is clear from the last Figure that all gains didn't have a clear difference in undershooting (peak) value, TVIWPSO gives the best minimum overshoot value and the best gain according to settling time are for MAACPSO then CPSO.

LFC WITH INTEGRAL CONTROLLER (WITH GRC)

With the same model parameters as illustrated in section 5.4.1.1 but in addition to ΔP_L = 0.01 p.u and GRC (-0.1/60) as shown in Figure 16.

The Figure 17 illustrates the frequency deviation comparison between different PSO gains of a single area with Integral controller with using GRC.

It's clear from Figure 17 that all gains didn't have a notable difference in undershooting (peak) value, MAACPSO gain gives the best gain minimum first and second overshoot value while MAACPSO and AACPSO have the best value according to settling time.

Table 7. Performance and values of PID gain with different types of PSO

	K_p	K_i	K_d	Objective function	Settling time	Peak Value
TVIW PSO	0.1	29.365	24.57	0.001942	71.959	0.002292
CPSO	41.99	53.373	99	0.0033515	72.125	0.002285
AAC PSO	24.66	82.001	79.69	9.6473e-024	72.239	0.002286
MAAC PSO	41.85	98.587	95.86	219.56	72.261	0.002285

LFC with Proportional–Integral–Derivative (PID) Controller with GRC

With the same model parameters as illustrated in 5.4.1.1 Section but in addition to ΔP_L = 0.01 p.u and GRC (-0.1/60) and using PID controller as shown in Figure 18.

Table 7 presents comparison performance and values of PID gain with different types of PSO.

The Figure 19 illustrates the frequency deviation comparison between different PSO gains of a single area with PID controller with GRC.

It is clear from Figure 19 that all gains didn't have a notable difference in undershooting (peak) value, while AAC PSO gives low overshoot its takes longer time than C PSO and MAACPSO, the gain of TVIWPSO gives the best value for settling time.

LFC with Automatic Voltage Control System

With the same LFC model parameters used in section 5.4.1.1 in addition to AVR model parameters:

$K_a = 10$, $T_a = 0.1$, $K_e = 1$, $T_e = 0.4$, $K_g = 0.8$, $T_g = 1.4$, $K_r = 1$, $T_r = 0.05$, $P_s = 1.5$, $K_2 = 0.2$, $K_4 = 1.4$, $K_5 = -0.1$, $K_6 = 0.5$,

In view of the fact that there is a weak coupling between LFC and AVR systems, so the frequency and voltage were controlled individually (see section 4).

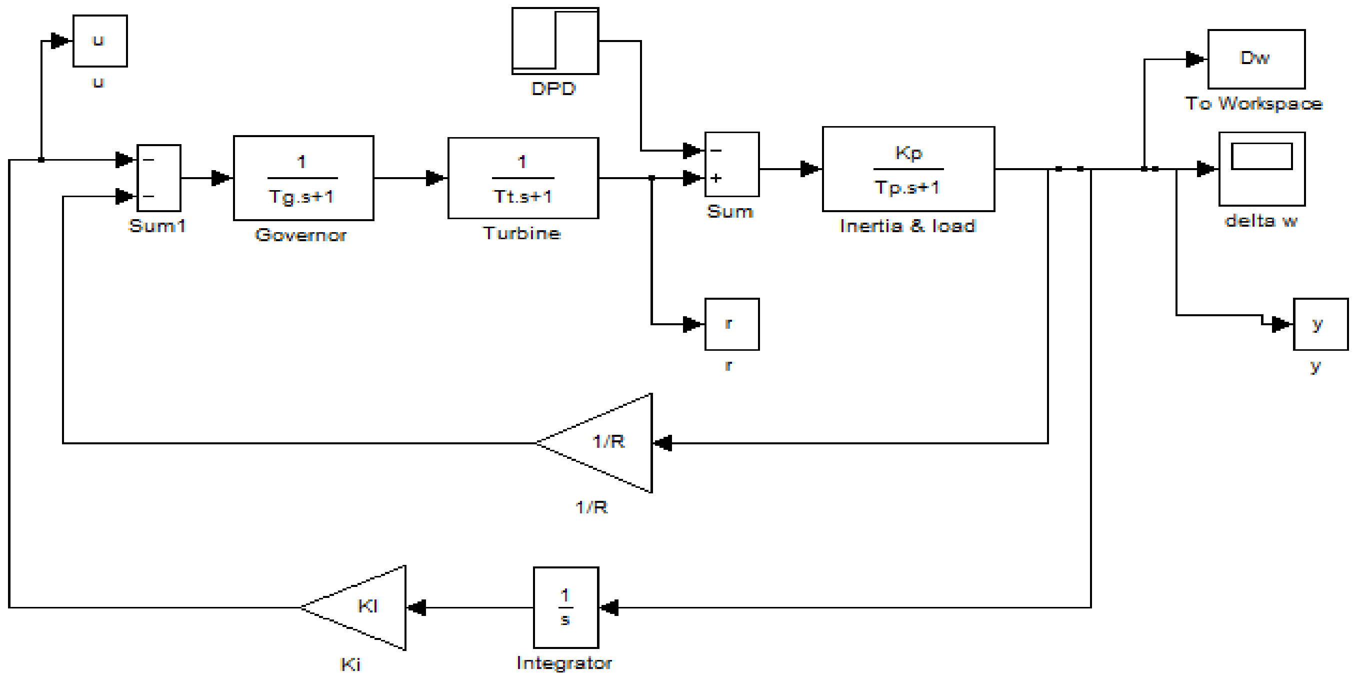

Figure 14. LFC Block Diagram.

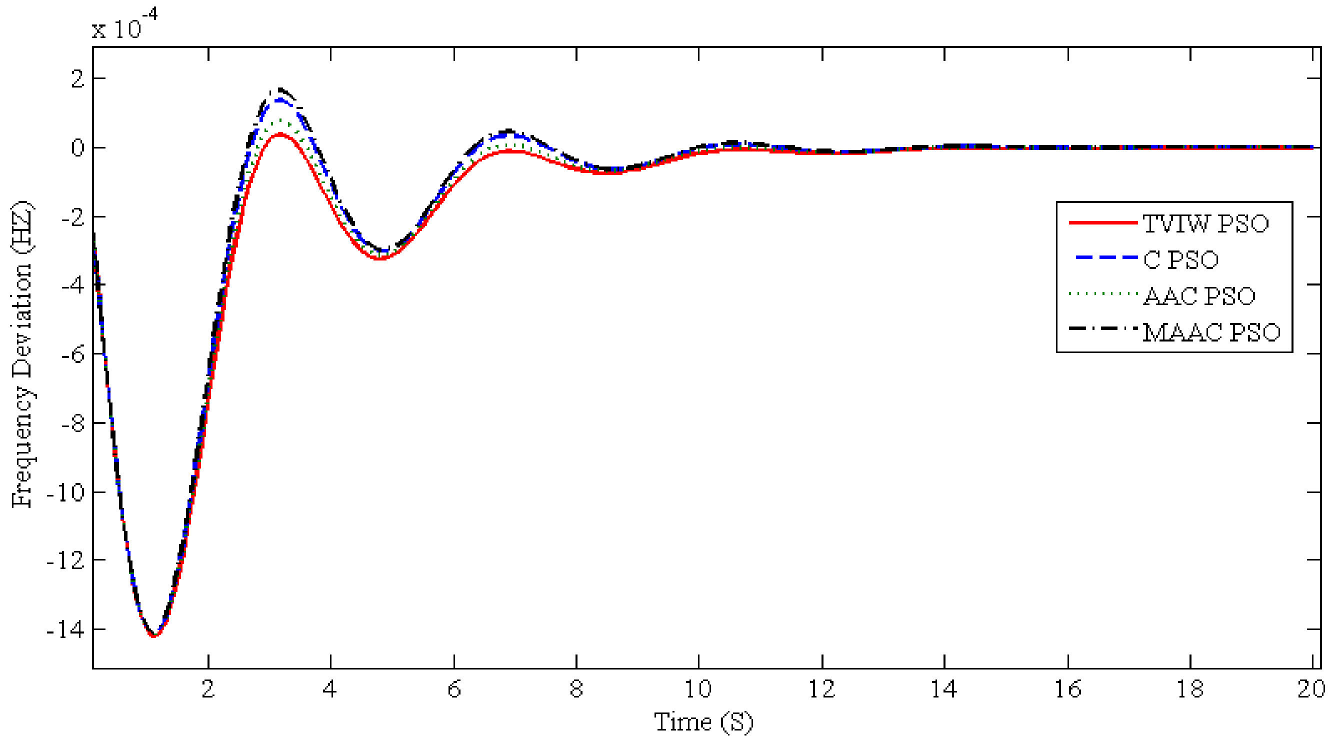

Figure 15. Frequency Deviation Comparison between different PSO gains of a single area with the integral controller without using GRC.

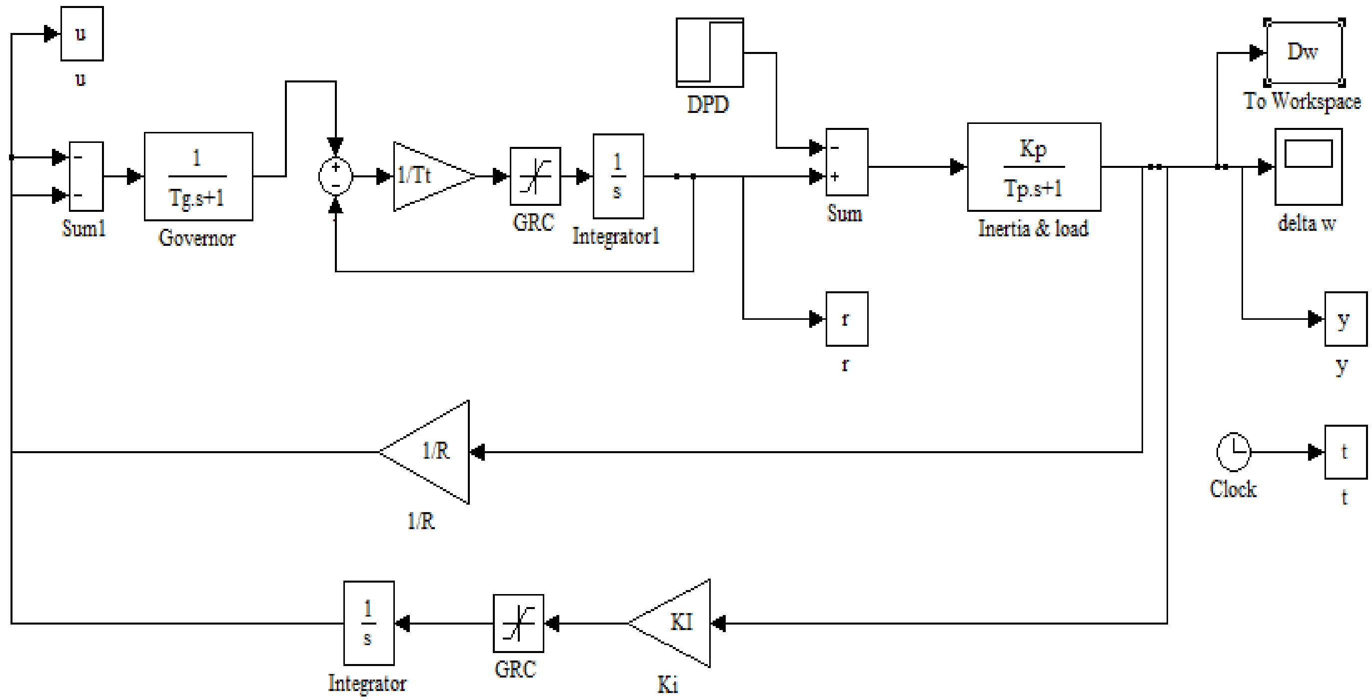

Figure 16. LFC with an integral controller with GRC.

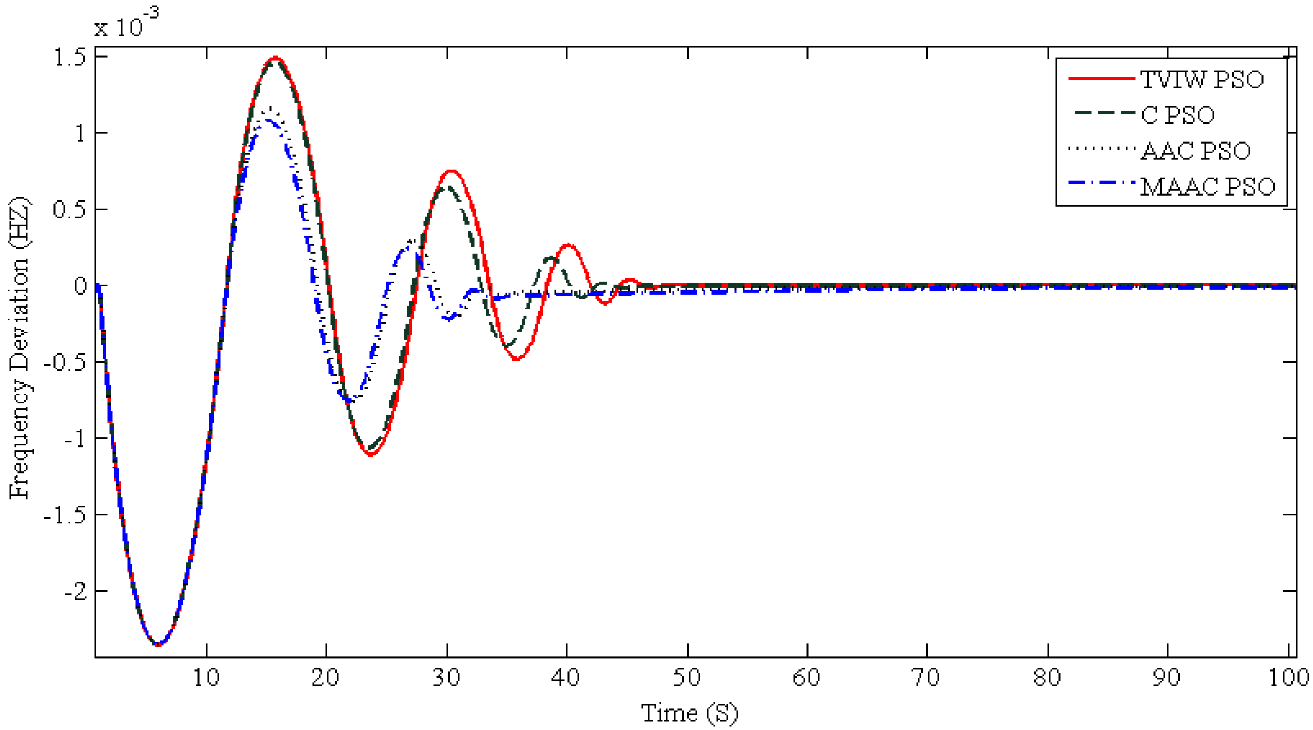

Figure 17. Frequency deviation comparison between different PSO gains of a single area with an integral controller with using GRC.

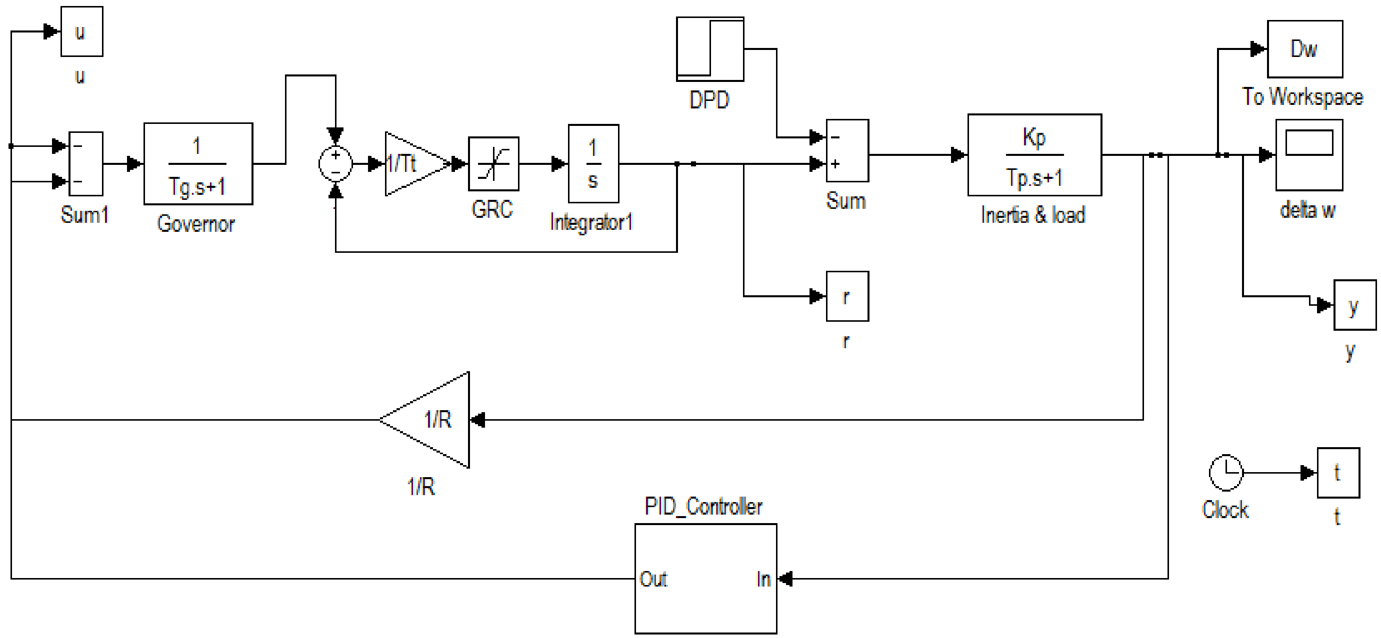

Figure 18. LFC with PID controller with GRC.

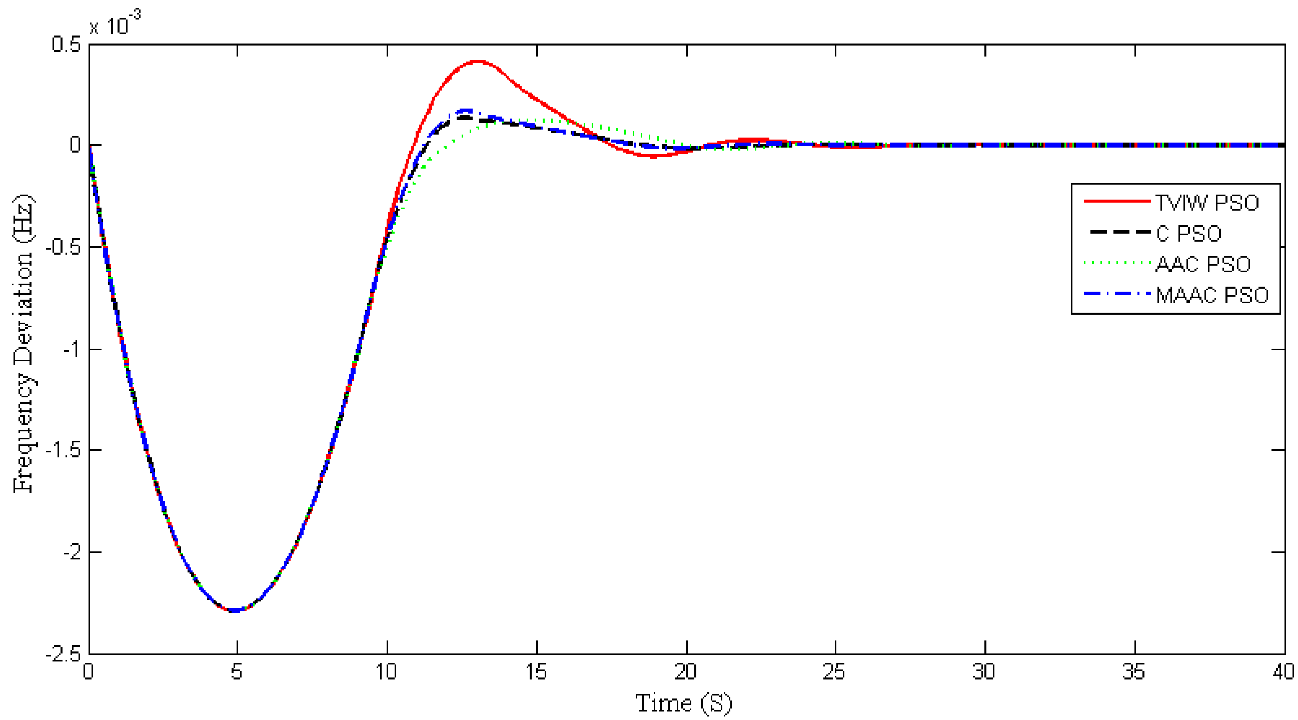

Figure 19. Frequency deviation comparison between different PSO gains of a single area with PID controller with using GRC.

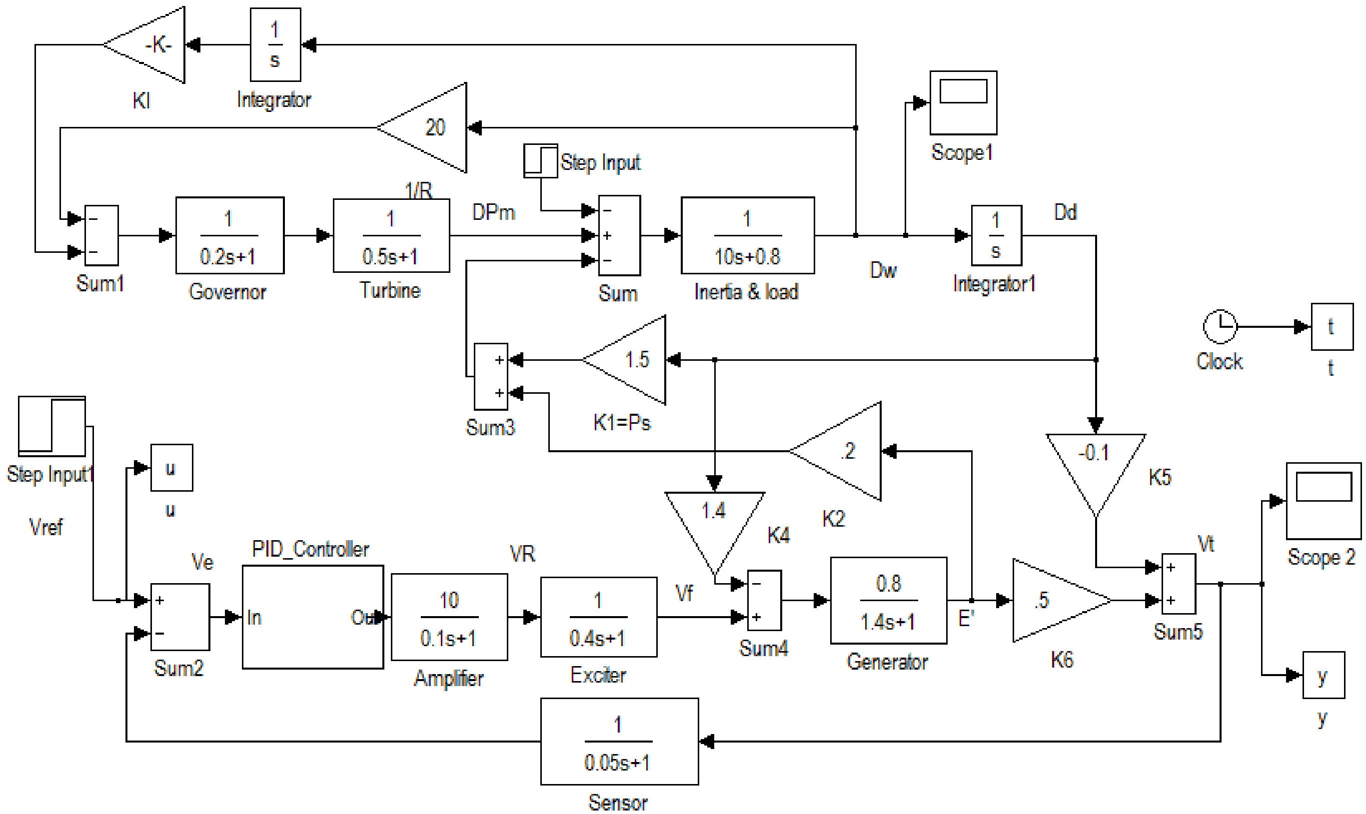

Figure 20. LFC with AVR block diagram using LFC integral gain without GRC.

LFC WITH AVR USING LFC INTEGRAL CONTROLLER (WITHOUT GRC)

With considering the parameters illustrated in Section 10.2, using an integral controller gain in LFC model compounded with AVR system as shown in Figure 20 with ΔP_L = 0.2 p.u and LFC integral gain = 6.4196 which produced from TVIWPSO LFC gain which is the best value at all (see section 9.1.1).

Table 8 illustrates Performance Evaluation for AVR-PID Controller Tuned by Different Types of PSO.

Table 8. Performance evaluation for AVR-PID controller tuned by different types of PSO

	K_p	K_i	K_d	Objective function	Rise time	Settling time	Peak value
TVIW PSO	3.7673	1.6077	1.5391	61.684	1.006	5.1159	1.0995
C PSO	3.4883	0.99936’	3.1713	664.43	2.052	5.1846	1.1176
AAC PSO	3.2549	1.6299	1.1944	940.87	0.9672	4.9801	1.1029
MAAC PSO	5.5723	1.3338	1.708	514.62	0.9564	5.3854	1.0719

The Figure 21 illustrates the terminal voltage step response comparison between different PSO gains of a single area with using the LFC-integral controller without GRC.

Figure 21 shows that CPSO gain takes longer rise time and settling time compared with other gains, the MAACPSO gain value gives the best settling time and less overshoot peak value compared with other gain values.

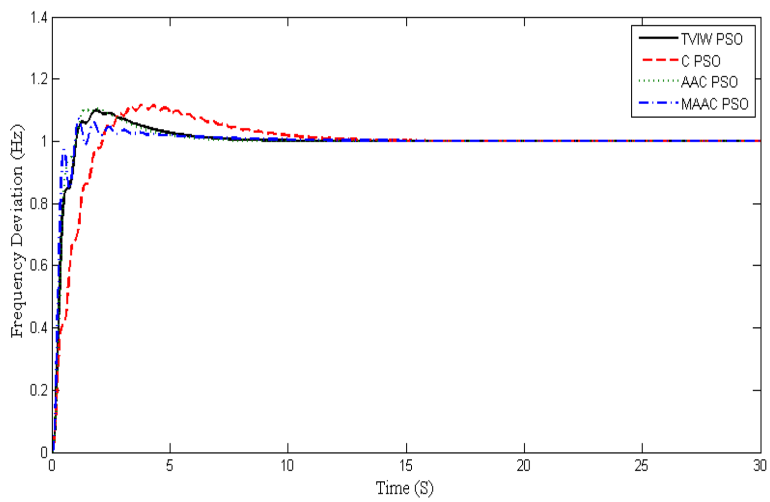

Figure 21. Terminal voltage step response comparison between different PSO gains of a single area with using the LFC-integral controller without GRC.

SINGLE AREA LFC/AVR USING AN INTEGRAL CONTROLLER (WITH GRC)

With considering the parameters shown in Section 10.2, using an integral controller gain in LFC model compounded with AVR system with GRC as presented in Figure 22 with ΔP_L = 0.01 per unit and LFC integral gain = 0.5765 which produced from MAAC PSO for LFC gain which is the best value at all, (see Section 10.1.2) and GRC equal (-0.1/60).

Table 9 gives a Comparison Performance and Values of AVR-PID Gain with Different Types of PSO.

The Figure 23 presents the terminal voltage transient response for a single area power system equipped with PID controller tuned by different types of PSO.

It obvious from Figure 23 that AAC PSO gain value gives the best value overall gains according to rise time,overshoot (peak) and settling time.

Table 9. Comparison performance and values of AVR-PID gain with different types of PSO

	K_p	K_i	K_d	Objective function	Rise time	Settling time	Peak value
TVIWPSO	4.7358	2.2877	2.3695	2158.45	0.9297	5.3068	1.1391
CPSO	7.7519	1.1941	2.3824	44.764	0.9564	5.6047	1.0991
AACPSO	3.9062	0.1943	2.7047	57.268	3.505	5.2517	1.0002
MAACPSO	3.731	1.3747	0.8119	5066.5	0.4836	5.0691	1.1925

SINGLE AREA LFC/AVR USING PID CONTROLLER WITH GRC

With considering the parameters shown in Section 10.2, using an integral controller gain in LFC model compounded with AVR system with GRC as presented in Figure 24 with ΔP_L = 0.01 p.u and LFC (PID) gain equal (K_p = 41.997; K_i = 53.373; K_d = 99) which produced from CPSO LFC gain which is the best value at all (see section 10.1.3) and GRC equal (-0.1/60).

The Table 10 presents a comparison performance and values of AVR-PID gain with different types of PSO.

Figure 25 shows that the CPSO gain gives the lowest overshoot gain value and the lowest value according to settling time is AACPSO gain while the rise time didn't have a major difference between all gains.

Table 10. Comparison performance and values of AVR-PID gain with different types of PSO

	K_p	K_i	K_d	Objective function	Rise time	Settling time	Peak value
TVIW PSO	3.5786	0.3199	0.815	17.2751	0.5282	6.4304	1.0847
C PSO	2	0.1396	1	7949.6	7.556	6.5577	1
AAC PSO	2.6385	1.0741	0.8864	23.733	0.8588	5.1021	1.0733
MAAC PSO	5.8704	0.4064	2.5104	58.84	1.414	7.4642	1.0095

RESULTS OF CASE STUDY IN MULTI AREA

This section introduces a simulation for the integrator and PID Controller in Load Frequency Control (LFC) in addition to Generation Rate Constraint (GRC) for Multi-area power system which containing two different area capability. For this purpose, MATLAB-Simulink software is used.

In section 10, results show that the PID controller gives the best performance respect to rising, settling times and overshoot. Also adding GRC model gives the simulation more non-linearity and complexity. According to this reasons, in this section and to aims to obtains controller deals with two area power systems, the study has used PID included GRC.

AGC AND AVR FOR TWO DIFFERENT AREA POWER SYSTEMS WITH GRC

The case under study is two area having two machines (generator and governor) of non-reheat steam turbines with different system parameters using PID controller for LFC model in each area and another PID for each AVR area with using GRC as shown in Figure 26, area 1 produced rated output is 250 MW and area 2 produced less than another area at supposed frequency is 50 Hz, sudden drop in load (Final value) in each area is 0.01 p.u and GRC in each area is (-0.1/60).

Construct AGC and AVR with GRC model and applying PSO algorithm MATLAB codes to optimize our problem to getting a suitable PID gain as shown in Figure 26.

Note that the PSO run simultaneously in both areas which mean the gains of one area related to another area to give the optimum result.

It’s noted that the initial drop load equal 0 and final drop load equal 0.01 with step time equal one.

Area 1 parameters:

Tg1 = 0.2	Kg1 = 1	Kt1 = 1	Tt1 = 0.5	H1 = 5	D1 =0.6	B1 = 20.6	K4 = 1.4
Ka1 = 10	Ta1= 0.1	Ke1 = 1	T1 = 0.4	Kg1 = 0.8	Tg1 = 1.4	K5 = -0.1	K6 = 0.5
Ps = 2 = K1	K2 = 0.2	Kr = 1	Tr = 0.05	1/R1 = 20	R1 = 0.05		

Area 2 parameters:

Tg2 = 0.3	Kg2 = 1	Kt2 = 1	Tt2 = 0.6	H2 = 4	D2 = 0.9	B2 = 16.9
R2 = 0.0625	Ka2 = 9	Ta2 = 0.1	Ke2 = 1	Te2 = 0.4	Kg2 = 1	Tg2 = 1
Kr2 = 1	Tr = 0.05	a12 = -1	1/R2 = 16	K8 = 0.5		

The Table 11 illustrates comparison performance and values of PID gains with GRC compared with different types of PSO.

The PID controller of AVR gains are $K_p = 2$; $K_i = 0.13967$; $K_d = 1$.

Table 12 presents comparison performance and values of LFC-PID gain with different types of PSO for the area (2).

The PID - AVR gains are $K_p = 2$; $K_i = 0.13967$; $K_d = 1$ (CPSO Gain from single area results, see section 10.2.3).

Table 11. A Comparison Performance and Values of LFC-PID gain with different types of PSO for Area (1)

	K_p	K_i	K_d	Objective function	Settling time	Peak value
TVIW PSO	0.05967	100	5.2412	517.181	66.1923	0.0909
CPSO	6.3119	44.133	8.1723	487.99	75.2692	0.0909
AAC PSO	0.2396	12.263	10	551.5611	67.2764	0.0909
MAAC PSO	4.9685	100	4. 6664	487.987	73.2223	0.0909

Table 12. A Comparison performance and values of LFC-PID gain with different types of PSO for the area (2)

	K_p	K_i	K_d	Objective function	Settling time	Peak value
TVIW PSO	9.6343	48.2654	9.1994	517.18139	61.5999	0.0833
CPSO	0.5	48.838	8.874	487.99	70.7152	0.0833
AAC PSO	15.252	36.1928	7.1996	551.5611	62.7517	0.0833
MAAC PSO	0.3403	23.7414	7.3120	487.9870	68.6351	0.0833

The Figure 27 displays comparisons between 4 gains for change in the frequency in the area (1).

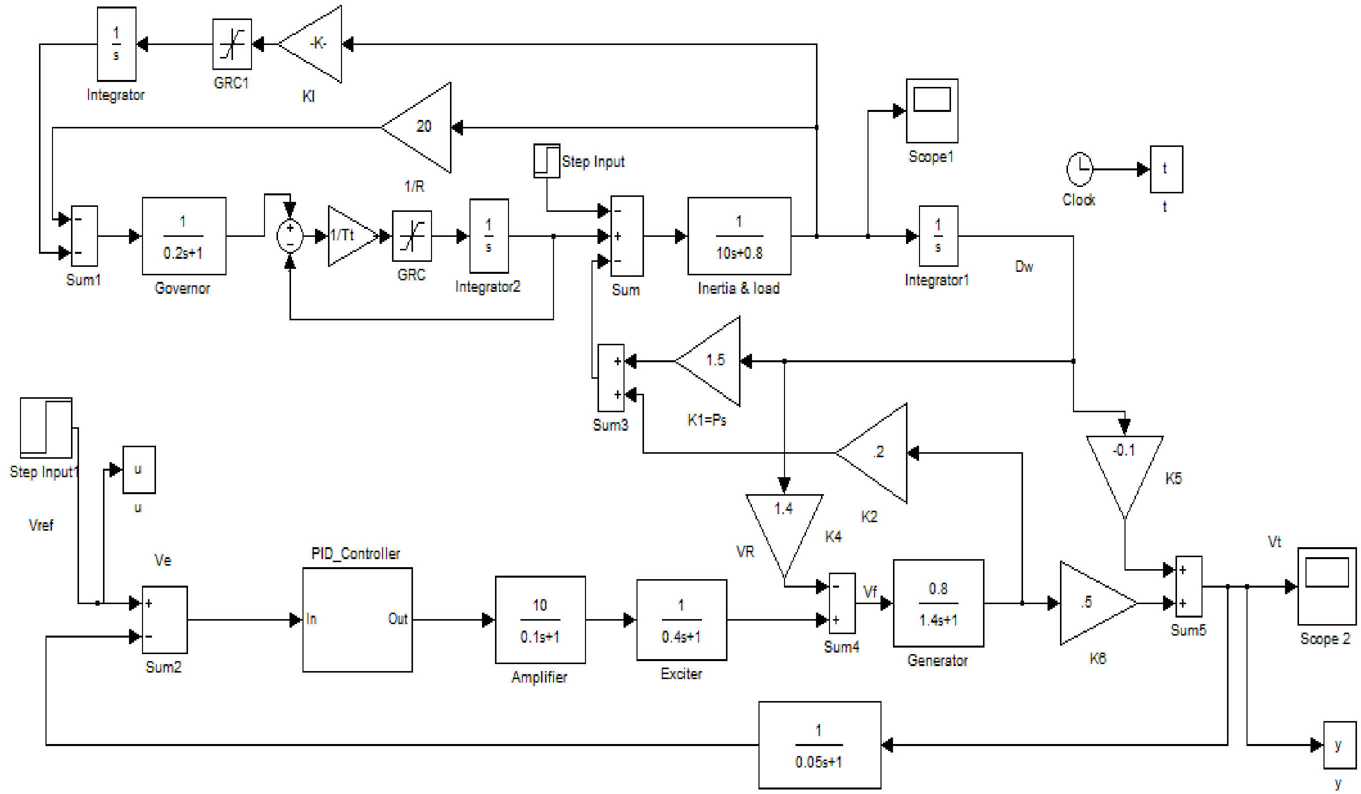

Figure 22. LFC with AVR block diagram using LFC integral gain with GRC.

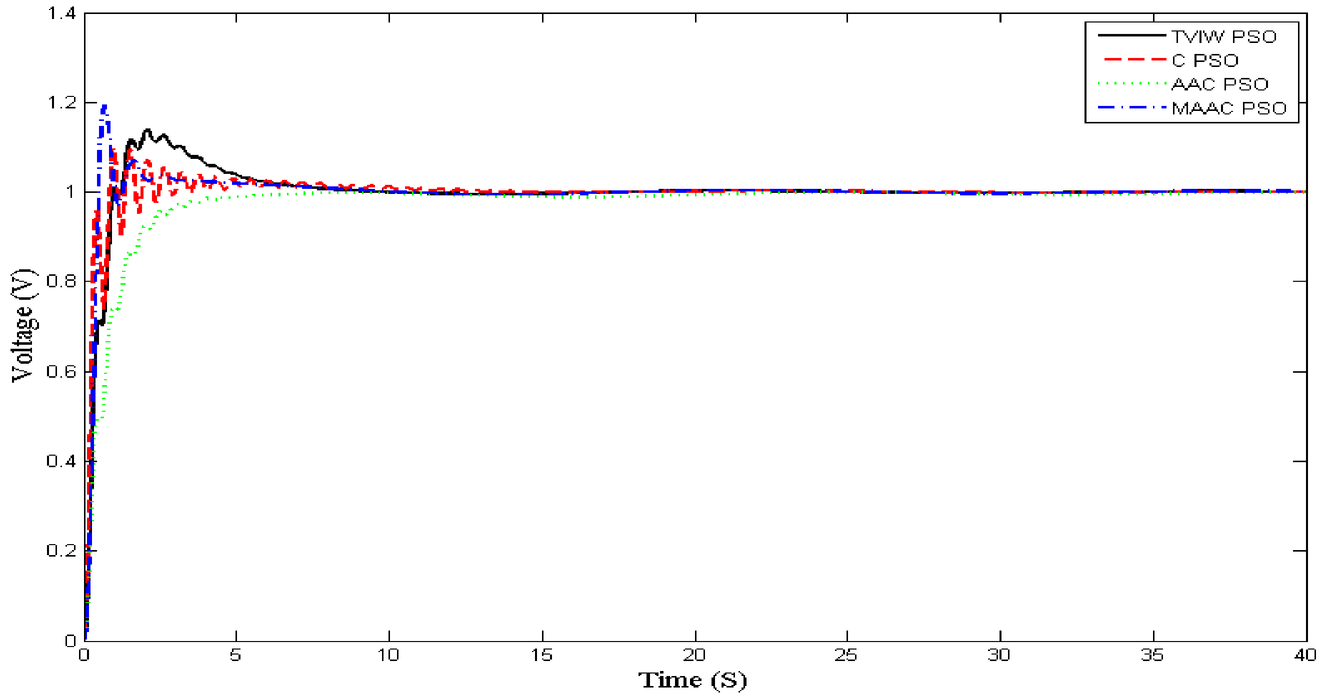

Figure 23. Terminal voltage step response comparison between different PSO gains of a single area with using an LFC-integral controller with GRC.

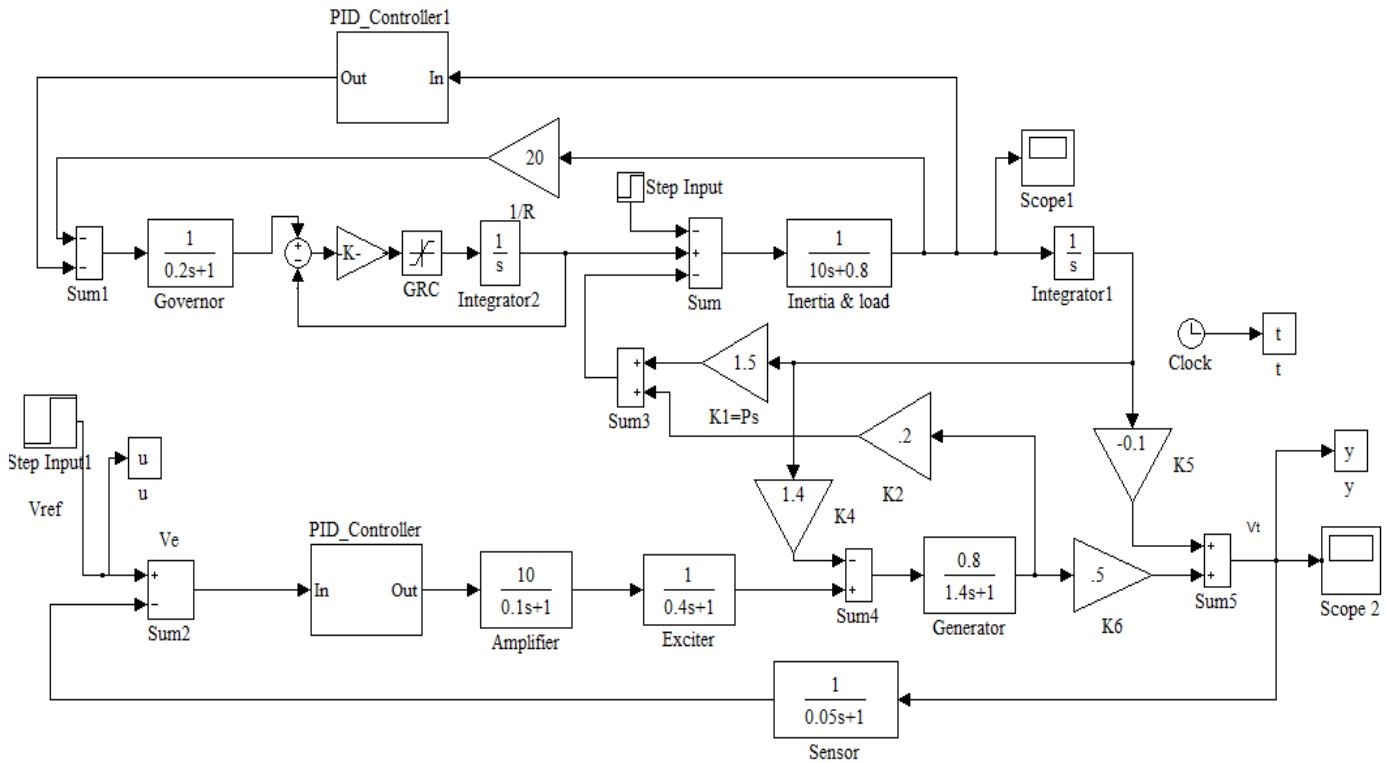

Figure 24. LFC with AVR block diagram using LFC- PID gains with GRC.

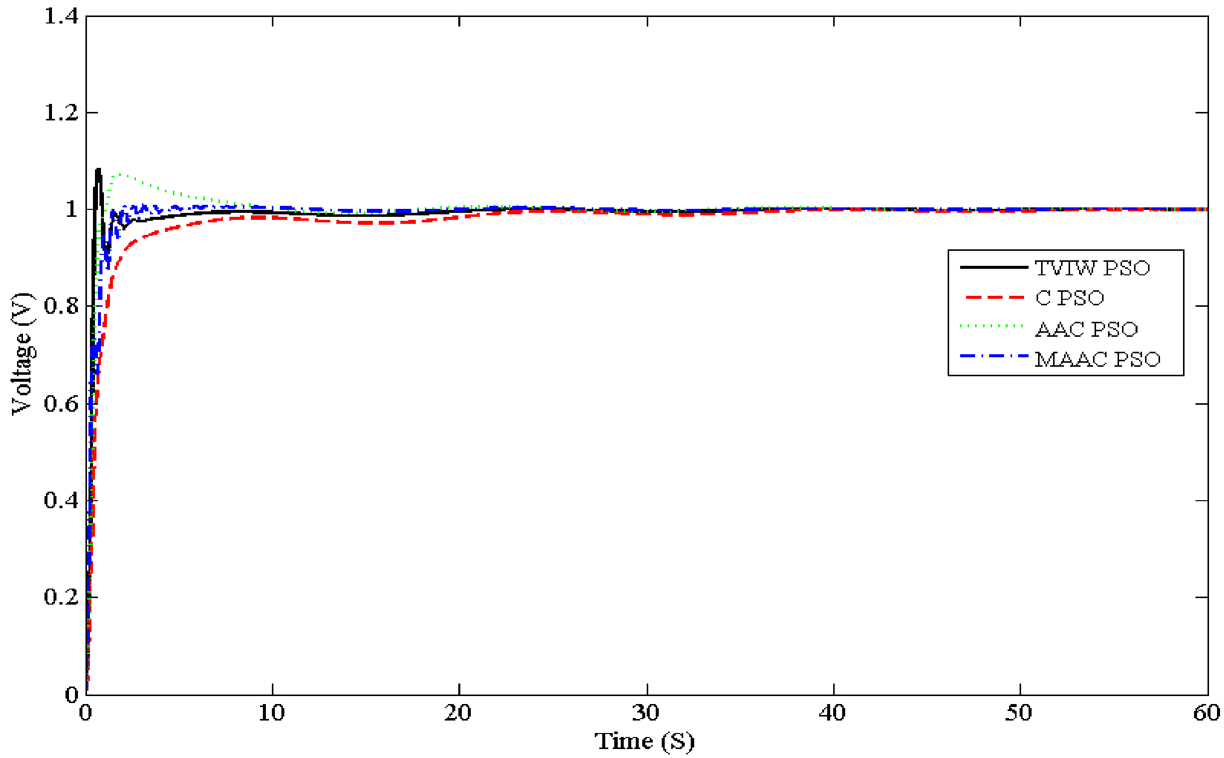

Figure 25. Terminal voltage step response compared with different PSO gains of a single area with using an LFC-PID controller with GRC.

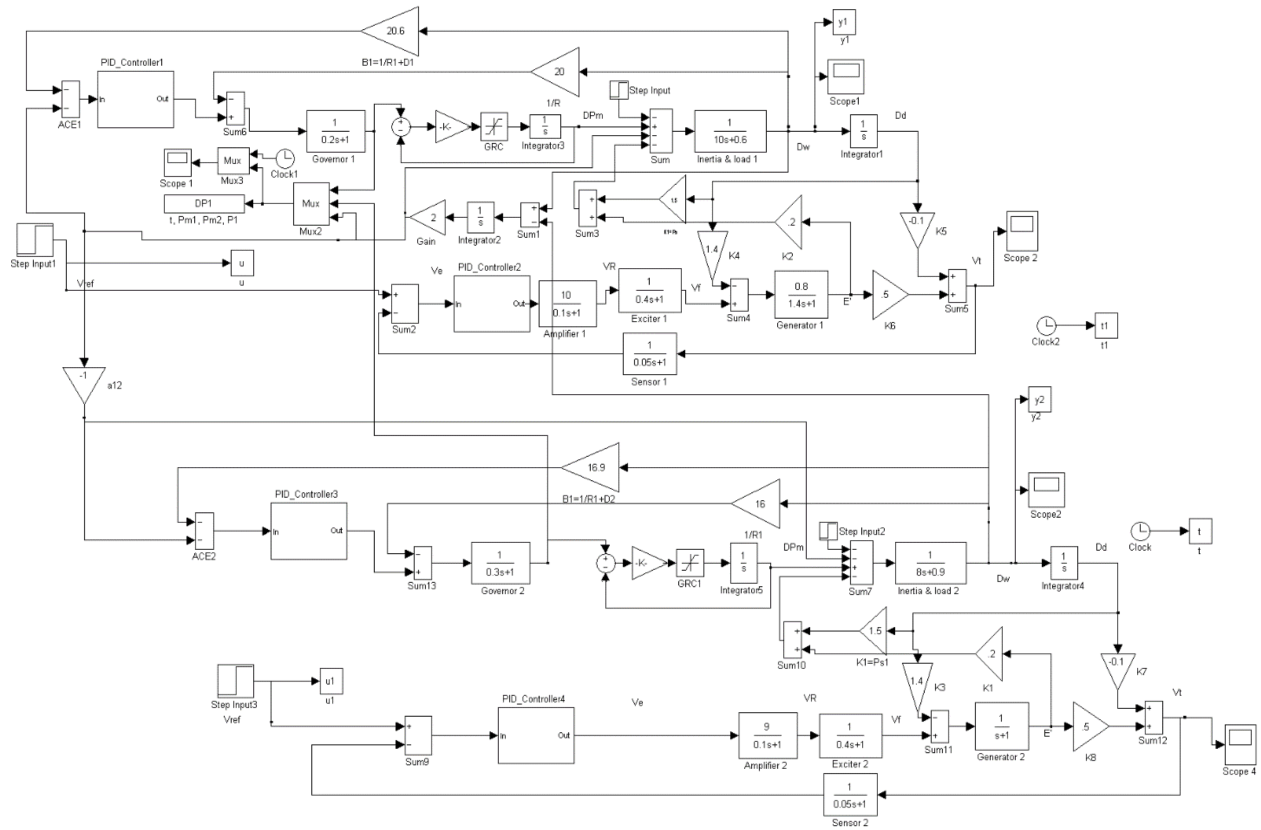

Figure 26. AGC-AVR block diagram of two different area power system included GRC.

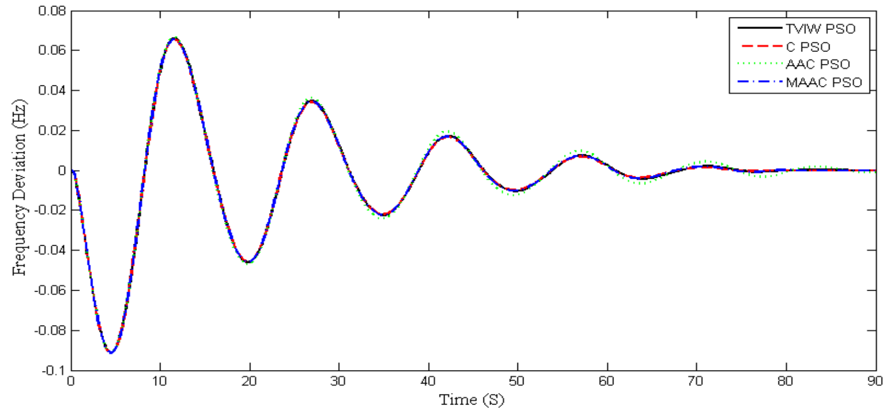

Figure 27. Comparisons between 4 gains for frequency deviation in the area (1).

The Figure 28 gives comparisons between 4 gains for change in the frequency in the area (2).

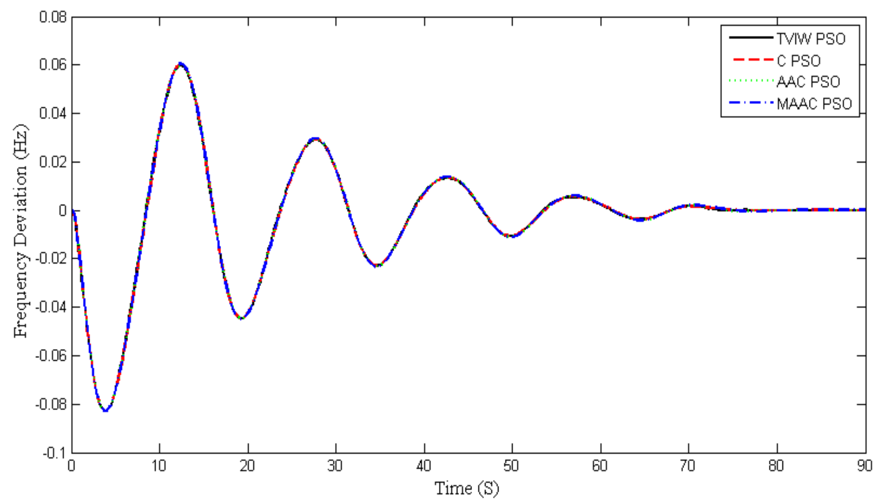

Figure 28. Comparisons between 4 gains for frequency deviation in the area (2).

It observed that all kinds of PSO used in this article didn’t give the big or obvious difference between them but even though, TVIWPSO gain seems it’s the best a little.

The Figure 29 displays the frequency deviation in the area (1) without using LFC and AVR controllers.

The Figure 30 gives the frequency deviation in the area (2) without using LFC and AVR controllers.

The Figure 31 illustrates frequency deviation in Area (1) with and without using LFC and AVR controllers.

The Figure 32 presents frequency deviation in Area (2) with and without using LFC and AVR controllers.

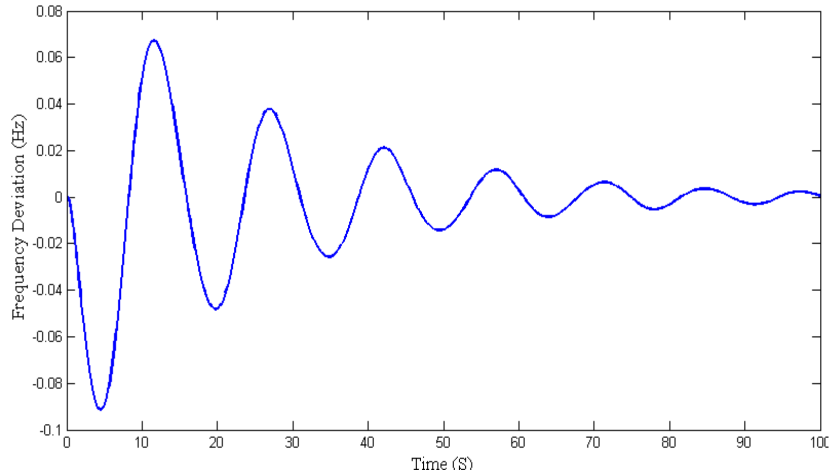

Figure 29. Frequency deviation in the area (1) without using LFC and AVR controllers.

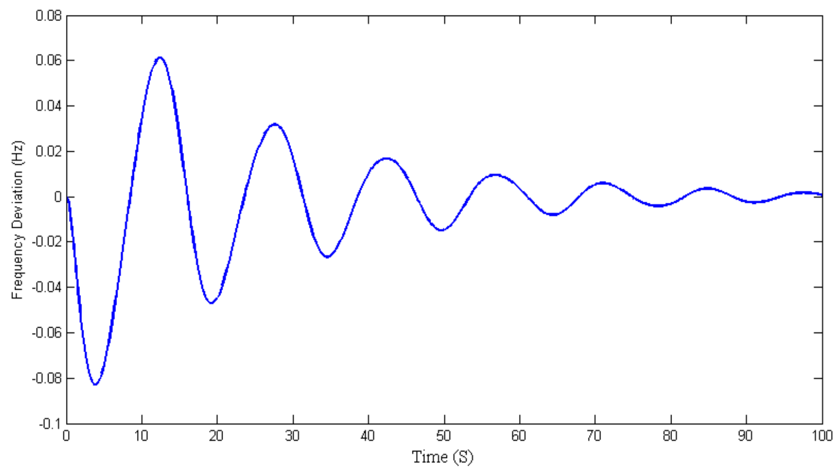

Figure 30. Frequency deviation in area (2) without using LFC and AVR controllers.

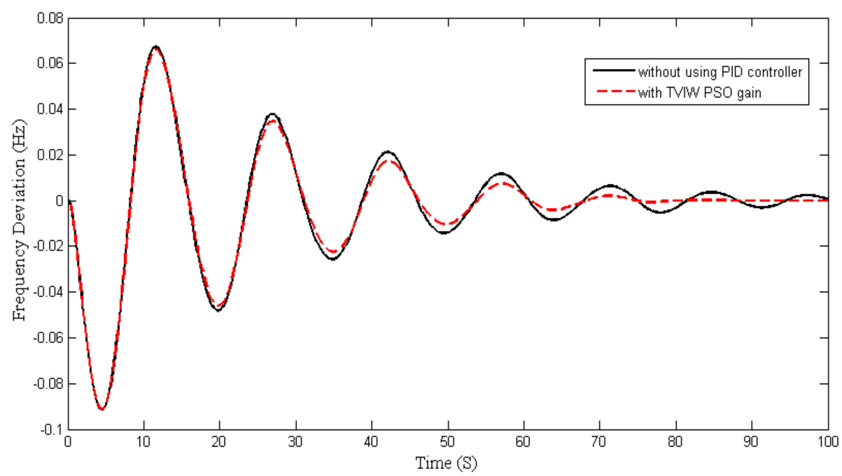

Figure 31. Frequency deviation in Area (1) with/without using LFC and AVR controllers.

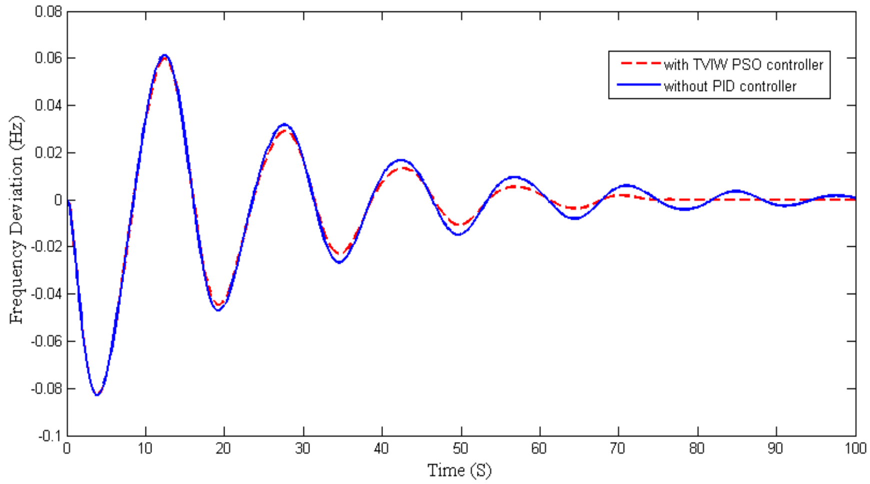

Figure 32. Frequency Deviation in Area (2) with/without using LFC and AVR controllers.

It's appearing from Figure 31 and 32 that TVIWPSO gain gives a good improvement in performance comparing without using the controller the difference.

SUMMARY AND CONCLUSION

Controlling the power system with achieving the requirements of consumers is a challenging task that inspires to design optimum controllers. The proposed controllers should have the capability of monitoring the power system frequency and voltage instantaneously. Many optimization techniques are discussed in the design of controllers. In this chapter, various types of evolutionary computation techniques were used to tune the parameters of hybrid I/PID controller equipped with LFC loop only and with both LFC and AVR loops. The simulation is applied for single and two area power system. GRC is taken into consideration to show the effectiveness of the proposed controllers.

The simulation results showed that the proposed Four Types of PSO were effective tools for LFC and AVR loops. It's evident from simulation results that the proposed PSO-based controllers enhanced the system dynamic performance.

CONTRIBUTIONS

The main contributions of the chapter are the following:

a) The obtained results showed the necessity for the additional control loop to improve the dynamic behavior of the systems equipped with it especially when system nonlinearity is considered.

b) A new simple and systematic method of designing integral and PID controller applied to power system dynamic problems. The new method elicited the design of integral and PID controller as an optimization problem and uses various types of PSO in the design procedure.
c) Linear and non-linear models of the surveyed systems were considered.
d) The robustness of the proposed controllers was discussed. It has been found that the proposed controllers by four types of PSO are almost insensitive to system parameters variations.
e) The effectiveness of the suggested controllers with regard to the expansion of loads and generating units has been tested. The four proposed controllers, in this chapter, have marked good dynamic response.
f) A new suggestion of PSO called Modified Adaptive Acceleration Coefficients (MAAC-PSO) gives tightness and robust performance for the cases study.
g) The proposed controllers tuning by different PSO reduce the effect between LFC and AVR and enhance the dynamic behavior of systems.
h) Construction of a two area model which has two different capability area power systems with a non-linear constraint then using various PSO to getting PID parameters.

FUTURE WORK

a) Suggesting new types of PSO to solve the frequency and voltage instability and power economic dispatch.
b) Applying the new types of PSO to power systems including renewable energy sources such as wind turbines and solar systems.
c) Applying these kinds in more than Two Area model.
d) Comparing MAACPSO with other EC Techniques (BAT Algorithms, Fire Fly, and ABC Algorithm).
e) Practical implementations of the proposed controllers in industrial applications.

ACKNOWLEDGMENTS

The authors gratefully acknowledge the support of the Ministry of Higher Education and Research, ASRT, STDF, and Benha University from Egypt. Ministry of Foreign and European Affairs, Ministry of Higher Education and Research, IRD, FCLAB, and UTBM from France (STDF-IRD Project #: 16330).

REFERENCES

[1] Gurdeepinder Singh, Rajni Bala. "Automatic Generation and Voltage Control of Interconnected Thermal Power System Including Load Scheduling Strategy" *International Journal of Engineering and Advanced Technology (IJEAT)* ISSN: 2249-8958, Vol. 1, No. 2, December 2011.

[2] Rakhshani, E., and Sadeh, J. Application of power system stabilizer in combined model of LFC and AVR loops to enhance system stability. *International Conference on Power System Technology (POWERCON), IEEE* No. 5940, pp. 1-5, October 2010.

[3] Ray, G., and Kumar, A. Decentralized adaptive PI control strategies for frequency control of interconnected systems. *Kybernetika*, Vol. 27, No. 5, pp. 458-478, 1991.

[4] Andersson, Göran. "Dynamics and control of electric power systems." *Lecture notes*, pp. 227-0528, 2012.

[5] Tammam, M. A., Moustafa, M. A., Ela, M. A., and Seif, A. E. A. Load Frequency Control Using Genetic Algorithm Based PID Controller For Single Area Power System. In: *International* (Vol. 12, No. 5).

[6] K. Yassin, E. Abd-Raboh, and M. S. Al-Domany "Fast Power Restoration Via Load Shedding Practices in Egyptian power System" *Mansoura Engineering Journal (MEJ)*, Vol. 17, No. 1, pp. 1-20, Mar. 1992.

[7] Ali, A. M., Ebrahim, M. A., and Hassan, M. M. Automatic Voltage Generation Control for Two Area Power System Based on Particle Swarm Optimization. *Indonesian Journal of Electrical Engineering and Computer Science*, 2(1), 132-144. 2016.

[8] Gozde, H., Taplamacioglu, M. C., and Kocaarslan, I. Application of artificial bee colony algorithm in an automatic voltage regulator (AVR) system. *International Journal on Technical and Physical Problems of Engineering*, Vol. 1, No. 3, pp. 88-92, 2010.

[9] Bhatt, V. K., and Bhongade, D. S. Design of PID Controller in Automatic Voltage Regulator (AVR) System Using PSO Technique. *International Journal of Engineering Research and Applications (IJERA)*, Vol. 3, No. 4, pp. 1480-1485, 2013.

[10] Omar, Bendjeghaba, and Ishak Boushaki Saida. "Bat Algorithm for Optimal Tuning of PID Controller in an AVR System." *International Conference on Control, Engineering and Information Technology (CEIT'14).* Proceedings. ISSN 2356-5608 pp. 158-1702014.

[11] Faiz, J., Shahgholian, G., and Arezoomand, M. Analysis and simulation of the AVR system and parameters variation effects, *POWERENG. International Conference on* IEEE in *Power Engineering, Energy and Electrical Drives*, pp. 450-453, 2007.

[12] M. A. Ebrahim et al. "Design of decentralized load frequency based-PID controller using stochastic particle swarm optimization technique." *Electric Power and Energy Conversion Systems, 2009. EPECS'09. International Conference on*. IEEE, 2009.

[13] M. A. Ebrahim et al. "Stochastic particle swarm optimization for tuning of PID controller in load frequency control of single area reheat thermal power system." *Int. J. Electr. Power Eng.*, 8(2), pp. 33-40, 2014.

[14] M. A. Ebrahim et al. "Optimization of Proportional-Integral-Differential Controller for Wind Power Plant Using Particle Swarm Optimization Technique." *International Journal of Emerging Technologies in Science and Engineering*, 2011.

[15] Mousa, M. E., M. A. Ebrahim, and Hassan, M. M. "Stabilizing and Swinging-Up the Inverted Pendulum Using PI and PID Controllers Based on Reduced Linear Quadratic Regulator Tuned by PSO." *International Journal of System Dynamics Applications (IJSDA)*, 4(4), pp. 52-69, 2015.

[16] Jagatheesan, K., Anand, B., Dey, N., and M. A. Ebrahim. "Design of Proportional-Integral-Derivative Controller Using Stochastic Particle Swarm Optimization Technique for Single-Area AGC Including SMES and RFB Units." In: *Proceedings of the Second International Conference on Computer and Communication Technologies* (pp. 299-309). Springer India, 2016.

[17] Javidan, J., and Ghasemi, A. A novel fuzzy RPID controller for multi-area AGC with IABC optimization. *Journal of Engineering*, 2013.

[18] Ali, E. S., and Abd-Elazim, S. M. Bacteria foraging optimization algorithm based load frequency controller for the interconnected power system. *International Journal of Electrical Power and Energy Systems*, Vol. 33. No. 3, pp. 633-638, 2011.

[19] Yousuf, M. S., Al-Duwaish, H. N., and Al-Hamouz, Z. M. PSO based nonlinear predictive control of single area load frequency control. In: *IFAC Workshop on Control Applications of Optimization*, May 2009.

[20] Babu, M. V. G., Hemanth, S. B., Kumar, S. T. S., and Prasanth, B. V. Single area load frequency control problem using particle swarm optimization. *International Journal of Electrical and Power Engineering*, Vol. 8, No. 1, pp. 1-6, 2014.

[21] Modi, N., Khare, M., and Chaturvedi, K. Performance Analysis of Load Frequency Control in Single-area Power System Using GA and PSO Based PID Controller. *International Journal of Electrical*, *Electronics ISSN*, pp. 2277-2626, 2013.

[22] AlRashidi, M. R., and El-Hawary, M. E. A survey of particle swarm optimization applications in electric power systems, *IEEE Transactions on Evolutionary Computation*, Vol. 13, No. 4, 913-918, 2009.

[23] Singh, S. N., and Yadagiri, J. Application of advanced particle swarm optimization techniques to wind-thermal coordination. *15th International Conference on* IEEE on *Intelligent System Applications to Power Systems, ISAP'09* (pp. 1-6), November 2009.

[24] Nápoles, G., Grau, I., and Bello, R. Constricted Particle Swarm Optimization based algorithm for global optimization. *Polibits*, 46, pp. 5-11, 2012.

[25] Mahor, A., Prasad, V., and Rangnekar, S. Economic dispatch using particle swarm optimization: A review. *Renewable and sustainable energy reviews*, Vol. 13, No. 8, pp. 2134-2141, 2009.

[26] Bo, Z., and Yi-jia, C. Multiple objective particle swarm optimization technique for economic load dispatch. *Journal of Zhejiang University Science A*, Vol. 6, Pt. 5, pp. 420-427, 2005.

[27] Ahmed, S., Tarek, B., and Djemai, N. Economic dispatch resolution using adaptive acceleration coefficients based PSO considering generator constraints, *International*

Conference on IEEE in *Control Decision and Information Technologies (CoDIT)*, pp. 212-217, May 2013.

[28] Gözde, H., Taplamacioğlu, M. C., Kocaarslan, İ., and Çam, E. Particle swarm optimization based load frequency control in a single area power system. *University Of Pitesti–Electronics and Computers Science Scientific Bulletin*, (8), pp. 1453-1119, 2008.

[29] Ratnaweera, A., Halgamuge, S., and Watson, H. C. Self-organizing hierarchical particle swarm optimizer with time-varying acceleration coefficients, *IEEE Transactions on Evolutionary Computation*, Vol. 8, No. 3, pp. 240-255, 2004.

[30] Eberhart, R. C., and Shi, Y. Comparing inertia weights and constriction factors in particle swarm optimization. In: *Evolutionary Computation*, *Proceedings of the Congress of IEEE*, Vol. 1, pp. 84-88, 2000.

[31] Birge, B. PSOt-a particle swarm optimization toolbox for use with Matlab. In: *Swarm Intelligence Symposium, (SIS'03) Proceedings of the IEEE* (pp. 182-186), May 2003.

[32] Rezazadeh, I., Meybodi, M., and Naebi, A. Adaptive particle swarm optimization algorithm for dynamic environments. In: *Advances in swarm intelligence*, Springer Berlin Heidelberg. pp. 120-129, 2011.